

Development of a reduced multi-component chemical kinetic mechanism for the combustion modelling of diesel-biodiesel-gasoline mixtures

Mohammad Zandie^a, Hoon Kiat Ng^{a,*}, Suyin Gan^b, Mohd Farid Muhamad Said^c,
Xinwei Cheng^d

^a Department of Mechanical, Materials and Manufacturing Engineering, University of Nottingham Malaysia, Jalan Broga, 43500 Semenyih, Selangor Darul Ehsan, Malaysia

^b Department of Chemical and Environmental Engineering, University of Nottingham Malaysia, Jalan Broga, 43500 Semenyih, Selangor Darul Ehsan, Malaysia

^c Automotive Development Center (ADC), Faculty of Mechanical Engineering, Universiti Teknologi Malaysia (UTM), 81310 Johor Bahru, Malaysia

^d School of Mechanical and Aerospace Engineering, Queen's University Belfast, Northern Ireland, UK

ARTICLE INFO

Keywords:

Chemical kinetic mechanism
Diesel-biodiesel-gasoline mixture
Mechanism reduction
Multi-component combustion mechanism

ABSTRACT

In this study, a compact combined reaction mechanism for diesel-biodiesel-gasoline mixtures (CDBG) is developed, comprising n-heptane, methyl butanoate (MB) and methyl decanoate (MD) as well as toluene and isooctane to represent the combustion characteristics of diesel, biodiesel and gasoline fuels, respectively. The mechanisms are separately reduced prior to combining by means of directed relation graph (DRG), directed relation graphs with error propagation (DRGEP) and full species sensitivity analysis (FSSA). The reduced mechanisms are then combined, and extensive validations are carried out for closed homogenous reactor application under the following conditions: $T = 600\text{--}1700\text{ K}$, $P = 1\text{--}50\text{ atm}$, and equivalence ratios (Φ) of 0.25–1.5 (156 setups in total). To boost the accuracy of the CDBG mechanism, cross-reaction analysis is performed to identify the important intermediate species and reactions. The identified species and reactions are subsequently integrated into the CDBG mechanism, resulting in significant improvements in ID timings up to 30%, 18% and 16% for the CDBG sub-mechanisms of diesel, biodiesel and gasoline, respectively. In addition, Arrhenius rate constant optimisation is also employed to further improve the ignition behaviour of the proposed kinetic mechanism. The results revealed that the dual implementation of the cross-reaction analysis and Arrhenius rate constant optimisation diminished the maximum associated errors considerably, down to 14.6%, 16.9% and 14.9% for the CDBG sub-mechanisms of diesel, biodiesel and gasoline, respectively. Concisely, the best results achieved at $T = 600\text{--}1700\text{ K}$ were $P = 41\text{ atm}$ and $\Phi = 1$, $P = 1,4\text{ atm}$ and $\Phi = 1$, and $P = 50\text{ bar}$ and $\Phi = 0.3$ for diesel, biodiesel and gasoline surrogates, respectively.

1. Introduction

The use of biodiesel in diesel engines adversely impacts the engine functionality and durability in the long-term due to its physicochemical properties [1]. Spray atomization and mixing issues caused by higher fuel viscosity, carbon deposition and adhesion of piston ring lead to problematic emissions control (particularly nitrogen oxide (NO_x)) and reduction in performance and service intervals biodiesel combustion in engines [2, 3]. Strategies to counter the abovementioned concerns include fuel preheating or using additives to enhance the combustion and emission characteristics of diesel-biodiesel blends have been proposed [4], but these inevitably reduce the commercial viability of

biodiesel. A more practically viable and feasible solution is to change the fuelling strategy by the addition of gasoline to resolve the fuelling reactivity associated with biodiesel fuels [5, 6]. This novel fuelling strategy has been reported to improve the overall functionality of diesel/biodiesel mixtures as well as engine performance under appropriate calibrations [7]. By adding gasoline, the combustion behaviour of diesel/biodiesel blends, particularly the ignition delay (ID) timing, is altered which provides more favourable air-fuel blending that ultimately controls the emissions [8]. The simultaneous reduction in NO_x and particulate matter (PM) has also been reported by the employment of gasoline cooperatively with exhaust gas recirculation and multiple injection techniques [9, 10].

* Corresponding author.

E-mail address: hoonkiat.ng@nottingham.edu.my (H.K. Ng).

<https://doi.org/10.1016/j.treng.2021.100101>

Received 3 October 2021; Received in revised form 26 November 2021; Accepted 18 December 2021

Available online 21 December 2021

2666-691X/© 2021 The Authors.

Published by Elsevier Ltd.

This is an open access article under the CC BY-NC-ND license

(<http://creativecommons.org/licenses/by-nc-nd/4.0/>).

To understand the combustion and emission characteristics of diesel-biodiesel-gasoline mixtures, both experimental and numerical analyses are needed. Numerical approaches are favoured over experimental studies, given the heavy demand and cumbersome time- and cost-related issues with the latter [11]. In the context of numerical research, surrogate models that are capable of replicating the combustion of actual fuels such as diesel have been proposed [12]. As such, to date, much research efforts have been expended on developing detailed chemical kinetic mechanisms that encompass a larger number of species and reactions found in the actual fuels. By incorporating chemical kinetic mechanisms into multi-dimensional computational fluid dynamics (CFD) modelling, engine-related phenomena such as the oxidation, ignition, combustion and emissions formation processes can be elucidated [13, 14]. However, despite the improvements achieved in computing power, it is still not practically viable to integrate such large detailed mechanisms into CFD simulations, due to the considerable required central processing unit (CPU) time and memory. The computational cost escalates by the third power of the species number, and the utilization of these detailed mechanisms can impose computational stiffness even for one-dimensional simulations [15]. Hence, amongst the available techniques to solve large detailed kinetic mechanisms, reduction techniques are more desirable particularly for 3D CFD simulations [16]. This apparent need for reduced mechanisms led to the development of mechanism reduction methods viz. directed relation graph (DRG) [17, 18] and dynamic adaptive chemistry (DAC) [19, 20]. Furthermore, the DRG method can also be combined with error propagation [21] and sensitivity analysis [22] techniques forming other reduction methods known as DRGEP and DRGEP-SA, respectively, which are used to further reduce the mechanisms and remove unimportant reactions and species.

Concerning diesel-biodiesel mixtures, a compact combined reaction mechanism was proposed by Ng et al. [1] via the combination of three-component mechanisms and a chemical class-based method. Their proposed mechanism contained the reaction schemes of methyl crotonate (MC) and methyl butanoate (MB) to account for the biodiesel surrogate and n-heptane as a surrogate for diesel. The final mechanism consisted of 80 species and 299 reactions and it was validated against 234 test conditions entailing pressures of 40–60 bar, initial temperatures of 750–1350 K and equivalence ratios of 0.4–1.5. Another multi-component mechanism applicable for simulating biodiesel, diesel and their blend fuels was introduced by An et al. [23] for biodiesel combustion in diesel engine, which comprised of methyl decanoate (MD), methyl-9-decanoate (MD9D) and n-heptane. The mechanism consisted of 112 species participating in 498 reactions in conjunction with the necessary mechanisms for carbon monoxide (CO), NO_x and soot formations. Extensive validations were conducted for the proposed skeletal chemical kinetic mechanism for 0-D ignition delay (ID) testing and 3-D engine simulations. Other similar investigations concerning multi-component chemical kinetic mechanisms for diesel-biodiesel mixtures have also been reported in the literature [24, 25].

Moreover, Li et al. [26] developed a chemical kinetic mechanism suitable for modelling studies on dual- and blend-fuel combustion of diesel-gasoline and biodiesel-gasoline in internal combustion (IC) engines. They integrated the chemical kinetic mechanisms of n-heptane, isooctane, MD and MD9D in their study. The ID timing for each of the sub-mechanisms was validated individually under 102 conditions. The validated mechanism comprised of 107 species and 425 reactions. Subsequently, the developed multicomponent mechanism was further validated under three-dimensional modelling under both single and double injection strategies of the respective fuels. Another major work in multi-component chemical kinetic mechanisms was conducted by Ren et al. [27], in which 11 components from six different classes of hydrocarbons were employed for the combustion and soot formation predictions of wide distillation fuel (WDF) covering gasoline, jet and diesel fuels. Their chemical mechanism consisted of 178 species and 758 reactions and it was extensively validated against experimental data for

the ID timing, laminar flame speeds, species mole fractions and combustion data of direct injection compression ignition (DICI) engines. Their proposed mechanism was not only validated for each pure component individually, but also for different surrogate fuels for gasoline, jet fuel and diesel fuel.

Furthermore, Zhong et al. [28] provided insights into the spray combustion and emission characteristics of biodiesel-gasoline blends using CFD simulations in a constant volume chamber. In their research, toluene reference fuel and n-hexadecane were integrated as surrogates for gasoline and hydrogenated catalytic biodiesel (HCB) fuel, respectively. Furthermore, they developed a reduced kinetic mechanism combined with a reduced polycyclic aromatic hydrocarbon (PAH) mechanism to model the HCB-gasoline soot formation and spray combustion. The accuracy of their proposed mechanism was benchmarked against the ID timing, liquid penetration length, lift-off length and soot formation. It was ascertained that their mechanism in conjunction with a multi-step phenomenological soot model could accurately replicate the spray characteristics and soot formation of the respective fuels under gasoline compression ignition (GCI) engine combustion conditions.

Nonetheless, in most of the investigations conducted on multi-component dual fuel surrogates that concerns the utilisation of reduced mechanisms, there is a lack of accuracy which is imposed by the elimination of important species and their associated reactions while being reduced. To this end, the integration of cross-reactions analysis is viable to address this issue, where the free radicals produced by one fuel extract hydrogen ions from another existing fuel in the mixture are recognised during the oxidation process and added to the reduced mechanism. As such, Liu et al. [29] proposed a reduced multi-component chemical kinetic mechanism for a diesel-natural gas dual fuel engine using cross-reactions analysis. Their results revealed that the integration of cross-reactions noticeably enhanced the prediction accuracy of the ignition behaviour for the reduced mechanism particularly at low to medium temperatures. In addition, the optimisation of Arrhenius reaction rate constants is also proven to maintain the accuracy of the detailed mechanisms upon reduction. Poon et al. [30], for instance, utilised the Arrhenius parameters optimisation in their developed multi-component diesel surrogate fuel model and it was discerned that more accurate predictions of the ID timing and species concentrations were achieved under a diverse range of operating conditions. Henceforth, in this research, it is attempted to incorporate both the abovementioned methods to improve the accuracy of the developed mechanism.

The practical utilization of biodiesel fuels in the transportation sector still involves mixing with diesel fuels. However, since diesel fuels are non-renewable, the transportation sector will see increasing blends of biodiesels usage with time. Furthermore, the mixing of gasoline into diesel-biodiesel blends comes with some concerns such as the erratic combustion behaviour of gasoline mixtures under various loads that must be resolved to ascertain the optimum operating conditions. Therefore, there is a need for numerical investigations of the combustion behaviour of such mixtures before increasing the ratio of gasoline or biodiesel, to detect and resolve the challenges involved and achieve combustion reliability. Relating to this, the proposal of a robust and yet practically manageable multi-component chemical kinetic mechanism that can accurately capture the ignition behaviour of the respective mixture is of interest. Despite the advances attained in chemical kinetic mechanisms for dual fuelling strategies, there has not been a proposed multi-component chemical kinetic mechanism to study the combustion-related phenomena of diesel-biodiesel-gasoline mixtures. Therefore, in the present study, a novel compact diesel-biodiesel-gasoline (CDBG) reaction mechanism combined with cross-reactions analysis and Arrhenius reaction rate constants optimisation is developed to replicate the combustion-relevant phenomena of the respective blend under various operating conditions.

In this work, appropriate chemical kinetic mechanisms are selected under which the main combustion-related features of diesel, biodiesel

and gasoline fuels are accurately replicated, whilst, avoiding computational stiffness. As such, n-heptane, MB and MD and isooctane and toluene are utilised to emulate the ignition behaviour of diesel, biodiesel and gasoline fuels, respectively. Afterwards, the detailed mechanisms undergo multiple reduction methodologies individually, followed by combining the obtained reduced mechanisms into a merged mechanism. Subsequently, cross-reactions analysis and Arrhenius rate constants optimisation are investigated to further improve the ignition behaviour predictability of the multi-component mechanism. Lastly, a broad range of experimental data from the literature are extracted to ascertain the prediction capability of the developed multi-component CDBG mechanism at various temperatures, pressures and equivalence ratios for ID timing, flame speed and species mole fraction.

2. Development of the reduced CDBG kinetic mechanism

The development of the CDBG kinetic mechanism is comprised of four distinct stages, namely, the selection of appropriate chemical kinetic mechanism for each fuel, the mechanisms reduction procedure, the cross-reaction analysis and the Arrhenius rate constants optimisation. Each of the abovementioned steps is demonstrated in detail in the following sections, and for further clarity, a schematic of the implemented methodologies is illustrated in Fig. 1.

2.1. Chemical kinetic mechanisms assortments

The selection of integrated mechanisms must usually meet two important criteria. First, generally the size of the chosen mechanisms should not be too large so they can be employed for 3-D CFD modelling. This means that, attempting to fully replicate the actual fuel characterization will inevitably result in a rise in the complexity of the mechanism [29]. On the other hand, the intended mechanisms must be in close similarity with the target fuel in terms of its ignition characteristics [31].

The integration of surrogate mixtures is usually limited by the availability of reference species that can be found in the validated chemical kinetic mechanisms [32, 33]. An analysis of the potential surrogate models for emulating the thermophysical properties of diesel fuels have been conducted by Lin and Tavlarides [34]. amongst the available single-component surrogates, n-alkanes are widely utilized to represent the thermophysical properties of diesel fuels because they are the major components of diesel fuels and their oxidation processes are well-established [32]. N-heptane is a frequently employed surrogate to

represent the combustion behaviour of diesel fuels owing to its cetane number closeness to actual diesel fuels. One of the major works in chemical kinetic mechanisms development for diesel fuels was conducted at the Lawrence Livermore National Laboratory (LLNL) by Curran et al. [35], which has been employed extensively by other researchers to form reduced mechanisms [36, 37]. Another significant recent development of n-heptane kinetic mechanism has been carried out by the Chemical Reaction Engineering & Chemical Kinetics (CRECK) modelling research group, with the simultaneous integration of reaction mechanisms for soot formation and NO_x emissions under both low and high temperature conditions [38, 39]. Thus, to emulate the chemistry of diesel fuel, the n-heptane reaction mechanism comprising 654 species and 2827 reactions developed by the LLNL is employed [35, 40, 41].

As for biodiesel surrogate models, the kinetic mechanism of methyl butanoate (MB) has been utilised to reproduce the combustion kinetics of biodiesel fuels. Brakora et al. [42] utilised the combination of MB and n-heptane to emulate the methyl linoleate structure found in diesel-biodiesel mixtures. The size of the MB reaction mechanism is practically manageable to be used for 3-D CFD modelling [43]. However, the incorporation of the MB surrogate model was found to be insufficient to represent the carbonyl chain length of actual biodiesel fuels [16, 44], which led to inaccuracies in emulating the reactivity levels of biodiesels, especially for the negative temperature coefficient (NTC) region [45]. Henceforth, it was discerned that employing larger detailed mechanisms such as methyl decanoate (MD) and methyl-9-decanoate (MD9D) served to address the limitation of the MB surrogate [46, 47]. Therefore, the kinetic mechanism of MB developed by the CRECK modelling research group is adopted [48–50]. Meanwhile, the MD reaction mechanism has been previously investigated to replicate the chemical features of large-sized alkyl esters of biodiesels [16, 43, 51] whilst its reaction size is computationally viable to be employed [44]. Thus, the reaction mechanism of MD with 226 species and 5298 reactions from the CRECK modelling research group is also incorporated [48–50].

To replicate the physicochemical properties of gasoline fuels, the primary reference fuels (PRF) comprising n-heptane and isooctane are commonly used [6, 52]. The PRF surrogates can accurately capture the ignition behaviour of high paraffinic gasoline fuels, but fail to perform satisfactorily for high non-paraffinic gasoline fuels [53]. The reason behind this deficiency traces back to their zero sensitivity toward the research octane number (RON) and motor octane number (MON), whereas high non-paraffinic gasoline fuel possesses relatively high sensitivity [6, 53]. To this end, the combination of toluene, n-heptane

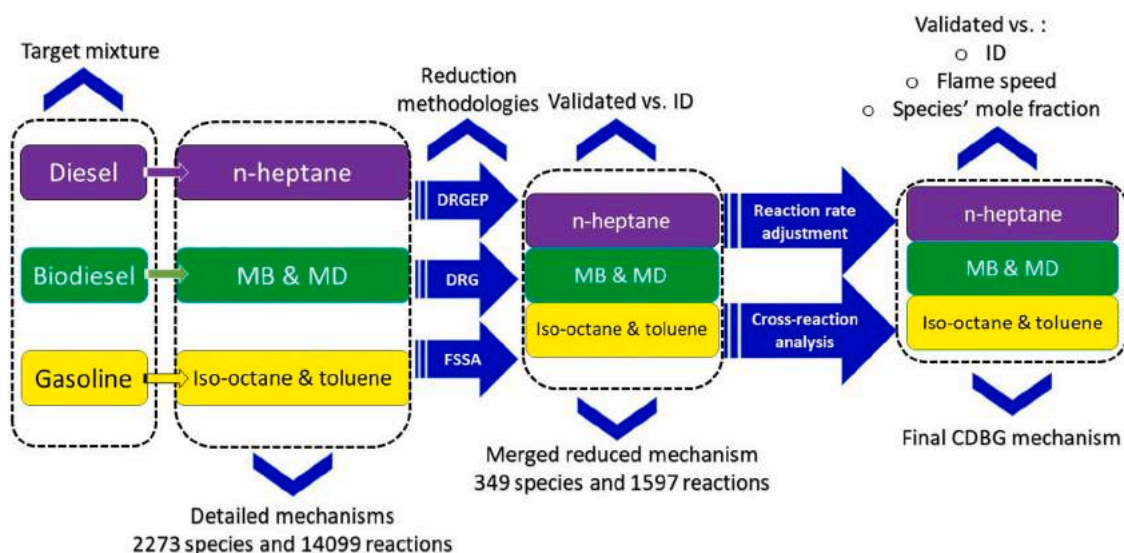


Fig. 1. Conceptual flow chart of the applied methodologies.

and isooctane known as TPRF has been developed to replicate the chemistry as well as the RON and MON sensitivities of actual gasoline fuels under a diverse range of conditions [53]. Thus, the kinetic mechanism developed by the LLNL research group for containing necessary species and reactions to account for the formation of important emissions such as NO_x and soot is selected in this work [40, 41, 54–57]. The incorporated mechanism contains 1393 species and 5974 reactions.

Over the years, the detailed multi-component mechanisms developed with higher number of species and reactions have been able to more accurately replicate combustion-related characteristics, when combined with other components [58]. For instance, the blend of TERF, which entails toluene, ethanol, isooctane and n-heptane was found to better emulate the ignition behaviour of gasoline [40, 59]. Also, the addition of n-dodecane and m-xylene was suggested as a multicomponent blend to accurately represent the combustion behaviour of diesel [60]. Besides, the blend of methyl palmitate (MHD), methyl stearate (MOD), methyl linoleate (MOD9D12D), methyl-5-decenoate (MD5D) and n-decane was recently proposed as a reliable skeletal oxidation surrogate mechanism for biodiesel [61]. Despite the availability of more complex detailed mechanisms, concerns remain regarding the computing resource and time needed to utilise such mechanisms. The higher the complexity of the integrated mechanisms, the higher the need for high-performance computers, particularly when it comes to 3-D simulations, thus leading to increased resource costs. On more affordable but lower specifications computers, the time taken for simulations using more complex mechanisms increases. Therefore, to date, practically manageable mechanisms in terms of computing power and time are still of high interest. For this reason, the mechanisms incorporated in this research are chosen as such to be feasible with the available computing power yet sufficiently accurate in predictions.

2.2. Reduction methodology

In this part, the utilised reduction methodologies are demonstrated in addition to their fundamental backgrounds. The purpose behind the mechanism reduction stage is to identify the species and reaction pathways with the least influential impacts on the overall performance of the mechanism, such that the associated complexities can be reduced whilst retaining the important features. The CHEMKIN-PRO Release

17.0 is used to perform the reduction methods, and in order to gain the best reduced mechanism, the DRGEP method is firstly applied on the mechanisms to identify redundant species, followed by the incorporation of the DRG method to further eliminate unimportant species and reactions [29]. Thereafter, the full species sensitivity analysis (FSSA) method is utilized to remove the remaining unimportant species. A schematic of the integrated reduction approaches is illustrated in Fig. 2.

It is worth pointing out that it is also viable to firstly merge the kinetic reaction mechanisms and then reduce the merged mechanism and vice versa [62–65]. Due to lack of sufficient experimental data for the simultaneous examination of diesel-biodiesel-gasoline mixtures, this study first reduced the mechanisms individually and then merged the obtained reduced mechanisms. Therefore, the sub-mechanisms of the final merged mechanism are benchmarked against their respective experimental data individually. Nonetheless, the opposite approach of merging first then applying the same reduction methodology was also tested and yielded a mechanism that requires an additional 23 species and 68 reactions to give relatively the same level of accuracy in terms of ID timing, flame speed and species mole fraction. Since the size of the mechanisms is of utmost importance, the former strategy is applied in this study.

2.2.1. Step 1: DRGEP technique

The DRGEP method integrates appropriate previous knowledge about the reaction system to detect the unimportant species present in the mechanism. Additionally, treating every species with different degree of significance will integrate the linking length between the coupling species. As such, as it is illustrated in Fig. 3, if species D is considered as an important species, species B and C will be deemed to have dissimilar contributions, bearing in mind the different connection lengths they possess to reach species D. Assuming two imaginary species as A and B, each species must be kept provided that when they are eliminated, a substantial error for the rate of production (ROP) of other species is imposed on the mechanism. This induced error is denoted as r_{AB} and is defined as follows [16, 29]:

$$r_{AB} = \frac{\sum_{i=1, I} |v_{A,i} w_i \delta_{Bi}|}{\sum_{i=1, I} |v_{A,i} w_i|} \quad (1)$$

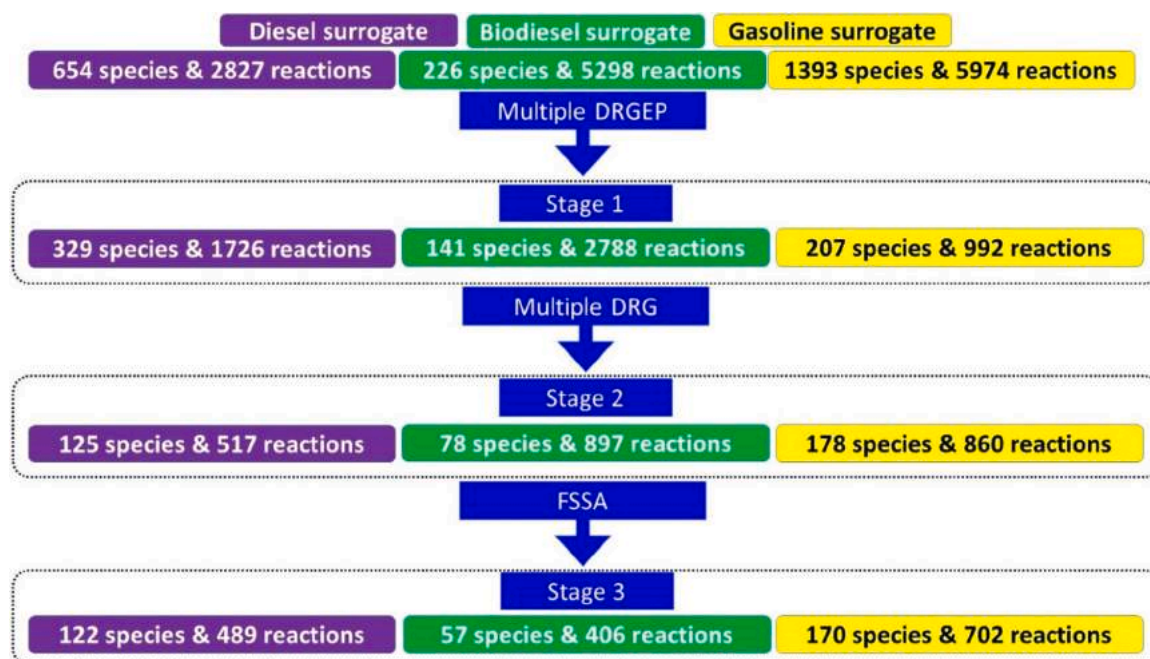


Fig. 2. Flow chart of the applied reduction methodologies and their corresponding reduced mechanisms.

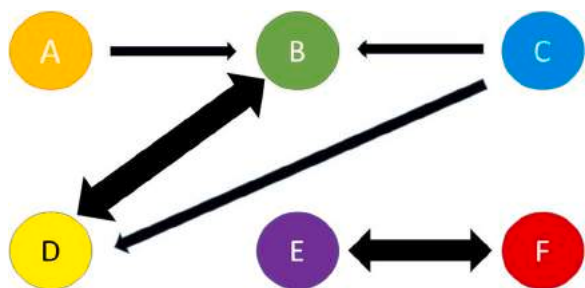


Fig. 3. A schematic of species relationship in DRG and DRGEP reduction methods.

which is subjected to two conditions as below:

$$\delta_{Bi} = \begin{cases} 1, & \text{if } B \text{ takes part in reaction } i \\ 0, & \text{otherwise} \end{cases} \quad (2)$$

$$R_A(B) = \max_s \{r_{ij}\}, \quad (3)$$

where A and B denote the intended species, i stands for the i^{th} reaction of the mechanism, $\nu_{A,i}$ illustrates the stoichiometric coefficient of the species A in the i^{th} reaction, δ_{Bi} indicates the existence ratio, and W_i represents the reaction rate of the i^{th} reaction. Also, the denominator signifies the total absolute contributions to the ROP of species A throughout all the reactions that encompass species A . In addition, the numerator denotes the contributions caused by the reactions involving species B as given in Fig. 3. Moreover, r_{ij} and S stand for the chain product of weights along with the reaction path of species A , and the set of all possible reaction paths from species A to species B , respectively. As depicted in Fig. 3, if species A is linked to another species as B , and B itself is in relation with another species as C , it is found that there is a link from species A to C through B . Therefore, in this approach if there is even one connection between species of A and B , in which its r value is higher than the user-defined threshold, species B must be retained in the reduced mechanism [29]. Once the component A is stored in the mechanism, all of the other components that could be achieved from component A (through either direct or indirect coupling) will be recognised via their $R_A(B)$ value as given in Eq. (3) [29].

Furthermore, the important species associated with the fuels, oxidizer (21% Oxygen (O_2), 79% Nitrogen (N_2)), and the complete combustion products (Carbon dioxide (CO_2), N_2 , and Water (H_2O)) have been considered throughout the reduction process as target species. Additionally, some extra components that play important roles in the oxidation process, such as OH , are also given to the system. It is also worthy to mention that the accuracy of the reduced mechanisms goes hand in hand with the user-defined error tolerance value. However, it is found that user-defined threshold value is not directly linked to the imposed error because the threshold error value does not always provide the least reduced mechanism [66]. The error tolerance for DRGEP was fixed to $1E-5$, hence, the species with lower r_{AB} than the user defined error tolerance will be eliminated from the mechanism. It is worthy to mention that the maximum allowable percentage errors throughout the reduction procedure was also fixed at 25% in order to obtain manageable-sized reduced mechanisms, but not at the expense of compromising the accuracy of the mechanisms too much.

As shown in Fig. 2, the DRGEP reduction approach was applied 4, 3, and 3 times on diesel, biodiesel, and gasoline surrogates, respectively, until no further reduction in mechanisms sizes was observed. It was discerned that the size of the associated species and reactions plunged sharply to 329 species and 1729 reactions for diesel surrogate, 141 species and 2788 reactions for biodiesel surrogate, and 207 species and 992 reactions for gasoline surrogate. This brought about significant mechanism size reductions of up to 49%, 38% and 85% species and 39%,

47%, and 83% reactions for diesel, biodiesel, and gasoline, respectively.

2.2.2. Step 2: DRG technique

The DRG method aims at detecting the least important species in a reaction mechanism by means of species coupling [17, 67]. It must be noted that on the contrary to the DRGEP approach, the DRG method takes no pre-known knowledge of the intended system [29]. The main assumption implemented in this technique is the idea of representing each species in the reaction mechanism using a distinct node, while the connections between the species are illustrated by vertices.

The Eqs. (1) and 2 are also applied in DRG method and once the value of r_{AB} is greater than a user-defined error tolerance, it can be perceived that the elimination of species B brings about an error to the ROP of species A ; henceforth, it must be kept in the reduced mechanism if species A is going to be kept in the mechanism. Moreover, provided that the exclusion of another species as C imposes a noteworthy error to the ROP of species B , the retaining of species A also requires the species C to be kept, due to the indirect coupling effects between species A and C .

The advantages obtained via the DRG method include, linear reduction time, manageable error and least user interaction throughout the process [16]. However, it is deemed that the DRG method treats all the species as of equal importance, and it may not be applicable for fast or low separation processes. Also, the DRG method is unable to recognize the inter-relation of species for nonchemical couplings and third bodies' impacts [16]. The reduction setups of DRGEP method are also integrated in the DRG method in this stage in terms of error tolerance value, target species and maximum allowable induced error. As it is shown in Fig. 2, after applying the DRGEP method, the DRG method was applied 2, 4, and 3 times on diesel, biodiesel, and gasoline surrogates, respectively. The results revealed substantial capability of the DRG method in reducing the mechanisms; concisely, 125 species and 571 reactions for diesel surrogate, 78 species and 897 reactions for biodiesel surrogate, and lastly 178 species and 860 reactions for gasoline surrogate were achieved. In other words, in comparison to the DRGEP outcomes, the DRG method resulted mechanism reduction size of up to 62%, 44%, and 14% species and 70%, 67%, and 13% reactions for diesel, biodiesel, and gasoline surrogates, respectively. At this point, further incorporation of the DRG method was not found to affect the mechanisms size, henceforth, the FSSA approach was then applied to probe any further mechanism reduction possibilities.

2.2.3. Step 3: FSSA technique

The rise in the complexity of the integrated mechanisms increases the level of difficulty in identifying the relative importance of each species present in the mechanism [29]. Hence, given the size of the detailed mechanisms utilised in this research, another approach to analyse the importance of chemical reactions is necessary. Species sensitivity analysis can provide deeper insights into the influential impacts of target pathways, which determine the outputs or products of the model, versus the change in particular parameters. If the intended results reveal a relatively greater degree of sensitivity to a primitive reaction pathway, then that reaction must be stored. Moreover, the predicted species concentrations and global properties have been reported to be sensitive to the uncertainties involved in the rate coefficients of the elementary reactions within the detailed chemical kinetic mechanisms [68].

Previous investigations authenticated that the size of reduced mechanisms produced by other methods such as the DRG approach can also be significantly influenced by the uncertainties in the rate coefficients [68, 69]. This was attributed to the fact that these methods eliminate the species via benchmarking the contributions of the production rates of important species from other species [68, 70]. Hence, for the sake of obtaining an optimum reduced mechanism, particularly in the uncertainty domain of reaction rate parameters, the species sensitivity analysis method is suitable to evaluate the importance of each species in the kinetic mechanisms and to simplifying them by

considering the input uncertainties [68]. Thus, in this research, the full species sensitivity analysis is used as the last stage, when no further reduction could be achieved via the previous two methods. The process of the FSSA method is briefly demonstrated below [29]:

- a The removal of individual species from reduced mechanisms that have been developed by previous reduction methods. This is followed by the calculation of the imposed error on the target factor for this removal.
- b Classifying the species versus the error they imposed on the system.
- c The removal of the species in ascending order (according to their error) and the calculation of the cumulative error they cause. The process breaks if the cumulated error increases further than a user-defined threshold.

To be more exact, throughout the species sensitivity analysis, each species is given a degree of importance (\bar{R}_s), and is classified into two bracket ranges as follows [63]:

$$\epsilon_{EP} < \bar{R}_s < \epsilon^* \quad (4)$$

$$\bar{R}_s > \epsilon^* \quad (5)$$

in which ϵ^* is a higher limit (e.g., 0.01–0.2), and those species that fall into the category of Eq. (4) are labelled as “limbo species” to be analysed separately for removal. Meanwhile, those which fall into the range given in Eq. (5) are classified as species to be retained in the reduced mechanism [63]. Afterwards, the error induced after the removal of each limbo species (\mathcal{R}_A) is evaluated by the sensitivity analysis algorithm, using Eq. (6):

$$\mathcal{R}_A = |\mathcal{R}_{A,ind} - \mathcal{R}_r| \quad (6)$$

where $\mathcal{R}_{A,ind}$ and \mathcal{R}_r are the error imposed by the removal of limbo species A and the error of the current reduced mechanism before omitting limbo species A, respectively [63]. In the next step, the sensitivity analysis algorithm categorises the species for removal in an ascending order using Eq. (6). Next, species removal is initiated and continues until the maximum error meets a user-defined limit. Therefore, those species whose elimination influences the reduced mechanism the least are the first to be selected for removal.

The integration of FSSA method as the last stage of the reduction process resulted in 122 species and 489 reactions for diesel surrogate, 57 species and 406 reactions for biodiesel surrogate, and 170 species and 702 reactions for gasoline surrogate, respectively. In other words, compared to the results gained from the DRG method, the FSSA method led to acceptable mechanism reductions of up to 2.4%, 27% and 4.5% species, and 5.4%, 55% and 18.3% reactions for diesel, biodiesel and gasoline surrogates, respectively.

2.3. Combination of the reduced kinetic mechanisms

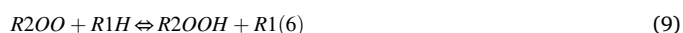
The merging sub-section of the Mechanisms Utilities Tool in CHEMKIN-PRO has been utilized to perform the merging process. It provides detailed analysis into differentiating the mechanisms details whilst allowing informed decisions to be taken during the combining procedure. As explained previously, the mechanisms for the fuels are separately reduced and then combined to form the merged mechanism. However, it is imperative to note that there are several approaches available to form the merged mechanism. The CHEMKIN-PRO allows merging two mechanisms at a time, and each time one mechanism is assumed as the master mechanism (base mechanism), while the other one is considered as the donor mechanism (to be merged). Afterwards, the software will identify common species and reactions within both the master and donor mechanisms. However, the Arrhenius parameters associated with these mutual reactions are not necessarily the same hence the user has the option to choose which mechanism, master or

donor, the Arrhenius parameters should be selected from. In this study, the Arrhenius parameters for the mutual reactions are selected from the master mechanism each time. Since this stage involves limitations, the future work recommendations for this stage are thoroughly stated in the limitation and future work section.

According to Fig. 2, the reduced mechanism of gasoline contains a higher number of species and reactions. Thus, it is considered as the base mechanism to combine with the other reduced mechanisms to form the CDBG mechanism [29]. The merging process has been carried out by firstly merging the biodiesel mechanism with the gasoline mechanism, followed by amalgamating the diesel mechanism with the merged biodiesel and gasoline mechanisms. Throughout the merging procedure, similar to detected mutual reactions, if two chemical species have similar chemical formula, then it is imperative to check their thermodynamic data (enthalpy, heat capacity and entropy at several temperature values). Provided that the thermodynamic data are analogous under different temperature values, then those species are considered identical, and the redundancy is removed [29].

2.4. Cross-reactions analysis

There are two dominant types of cross-reactions that distinguish them from other cross-reactions and chief components. The first class of cross-reactions is defined as the elementary reactions between small free radicals, such as the radicals of C1 to C3 and the active molecule of CO, which are formed by the oxidation cleavage reaction (as a part of the macro-molecule hydrocarbon structures in multi-component fuels) as well as between the macro-molecules and the active molecule of CO [29]. This type of cross-reactions plays a significant role in the middle and late phase of the oxidation process as well as the overall combustion, particularly as for the combustion of macro-molecules [71]. The second type of cross-reactions is deemed as the exchange of free radicals between the macro-molecules as a result of different macromolecules dehydrogenation. According to this definition, the typical cross-reactions can be categorised into three reactions as follows [29]:



From a theoretical standpoint, the lack of integrating these reactions would lead to almost half of the consumption rate not being considered [29]. Hence, an accurate combustion process modelling of multi-component mixtures requires a thorough consideration of such reactions.

The main species of cross-reactions are the secondary products of the fuels. In order to analyse the cross-reactions, the dominant intermediate species associated with the oxidation of each individual fuel is determined for the CDBG mechanism. As illustrated in Fig. 4, C7H15–3, C7H15–2 and PC4H9 components are the most important intermediate species throughout the n-heptane oxidation process owing to their relatively higher normalised sensitivities. Moreover, according to Fig. 5, RMDX, UME10, RUME10 and RMBX, CH2CO, CH3O, C2H4 are considered as the dominant intermediate species in the MD and MB oxidation processes, respectively. Lastly, as can be discerned from Fig. 6, C6H4CH3, C6H5CH2J, C6H4CH2OJ, YC7H15, YC7H15 and AC8H17 are the main intermediate species for the oxidation of toluene and isooctane, respectively. In addition, several other species that have revealed high normalised sensitivities for each fuel have also been integrated. The selected species and their associated integrated reactions are provided in Table 1.

Henceforth, the reactions between the abovementioned species are deemed as important cross-reactions that must be added to the CDBG mechanism. It is worthy to point out that although throughout the reduction stage it is possible to allow CHEMKIN-PRO to keep important

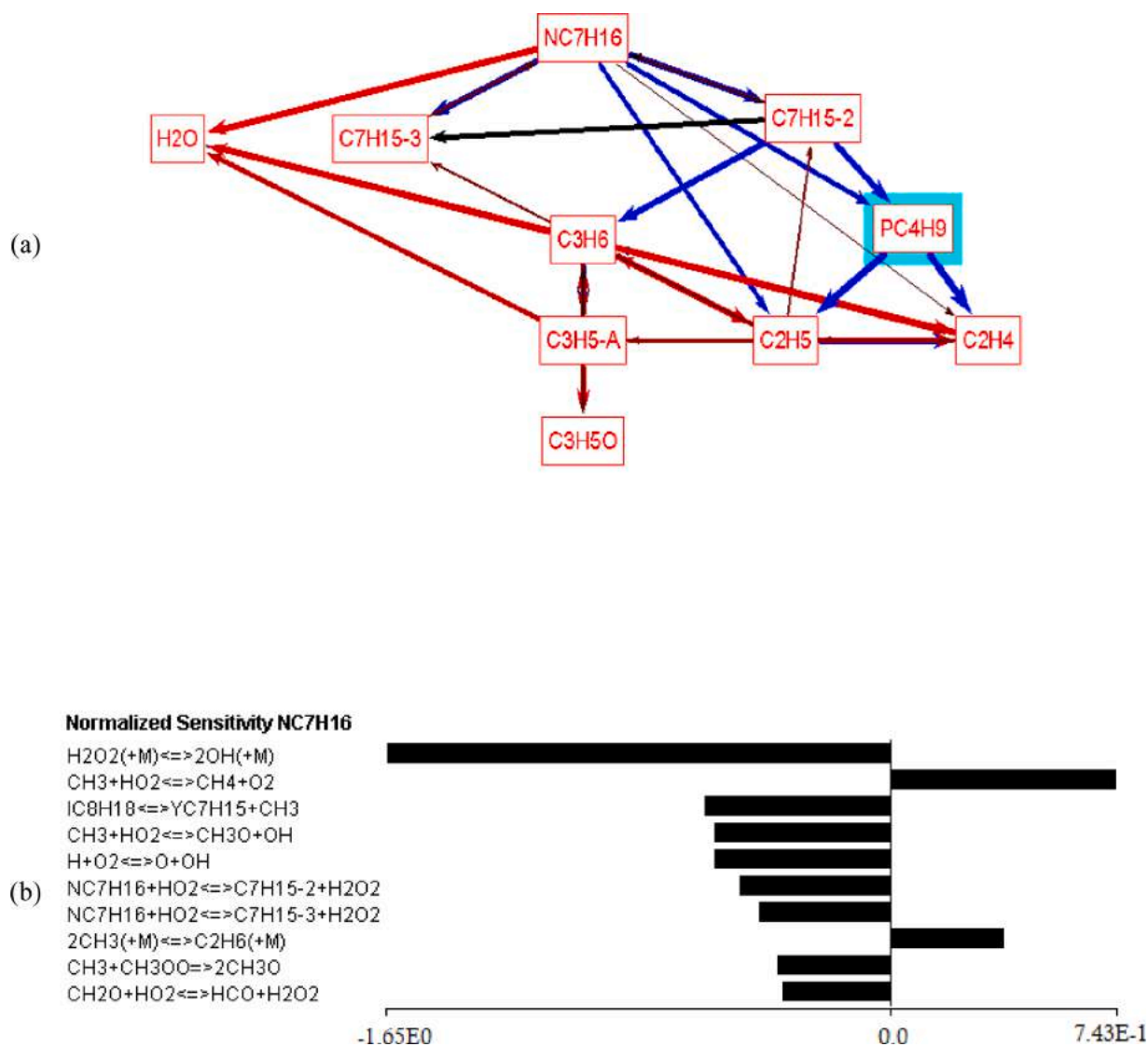


Fig. 4. Normalised combustion sensitivity and reaction path analysis of n-heptane.

predefined species, some reactions containing those species may be omitted. This is mainly because each fuel has been reduced individually, so some deleted reactions (due to low sensitivity on the overall combustion performance) may play significant roles once merged with other fuel mechanisms.

2.5. Optimisation of the Arrhenius rate constants

In addition to the cross-reactions analysis, another important technique known as the Arrhenius rate constants optimisation has also been used to further improve the prediction capability of the proposed CDBG mechanism. This method has been extensively utilised, particularly for multi-component kinetic mechanisms [43]. To this end, the reaction path analysis has been conducted to identify the important species and reactions for the particular operating conditions that the CDBG mechanism failed to provide more accurate predictions. This analysis was performed for each individual CDBG sub-mechanism, and then the detected reaction rates were optimised up to an acceptable degree. The identified important reactions with their corresponding original and adjusted reaction rate coefficients are presented in Table 2.

3. Results and discussion

Several validation procedures have been carried out to ensure the accuracy of the detailed, reduced and CDBG mechanisms in terms of ID timing prediction, flame speed and species mole fractions. Firstly, the validations of the reduced mechanisms versus detailed mechanisms and experimental data are presented. This is followed by the analysis into the effects of the cross-reactions method and the Arrhenius rate constants optimisation technique on the CDBG mechanism. Lastly, the validation of the CDBG mechanism equipped with cross-reactions and optimised Arrhenius rate constants for flame speed and species mole fractions predictions is detailed.

3.1. Validation of the reduced kinetic mechanisms

The ID timing has been considered for this stage to validate the accuracy of the reduced mechanisms for each individual fuel under a diverse range of conditions as given in Table 3. The experimental data (retrieved from the literature) for diesel and biodiesel fuels were conducted under shock tube (ST) conditions while rapid compression machine (RCM) data were used for gasoline fuel. Furthermore, the ID timing of both the detailed and reduced mechanisms have been predicted under closed homogenous batch reactor models using CHEMKIN-

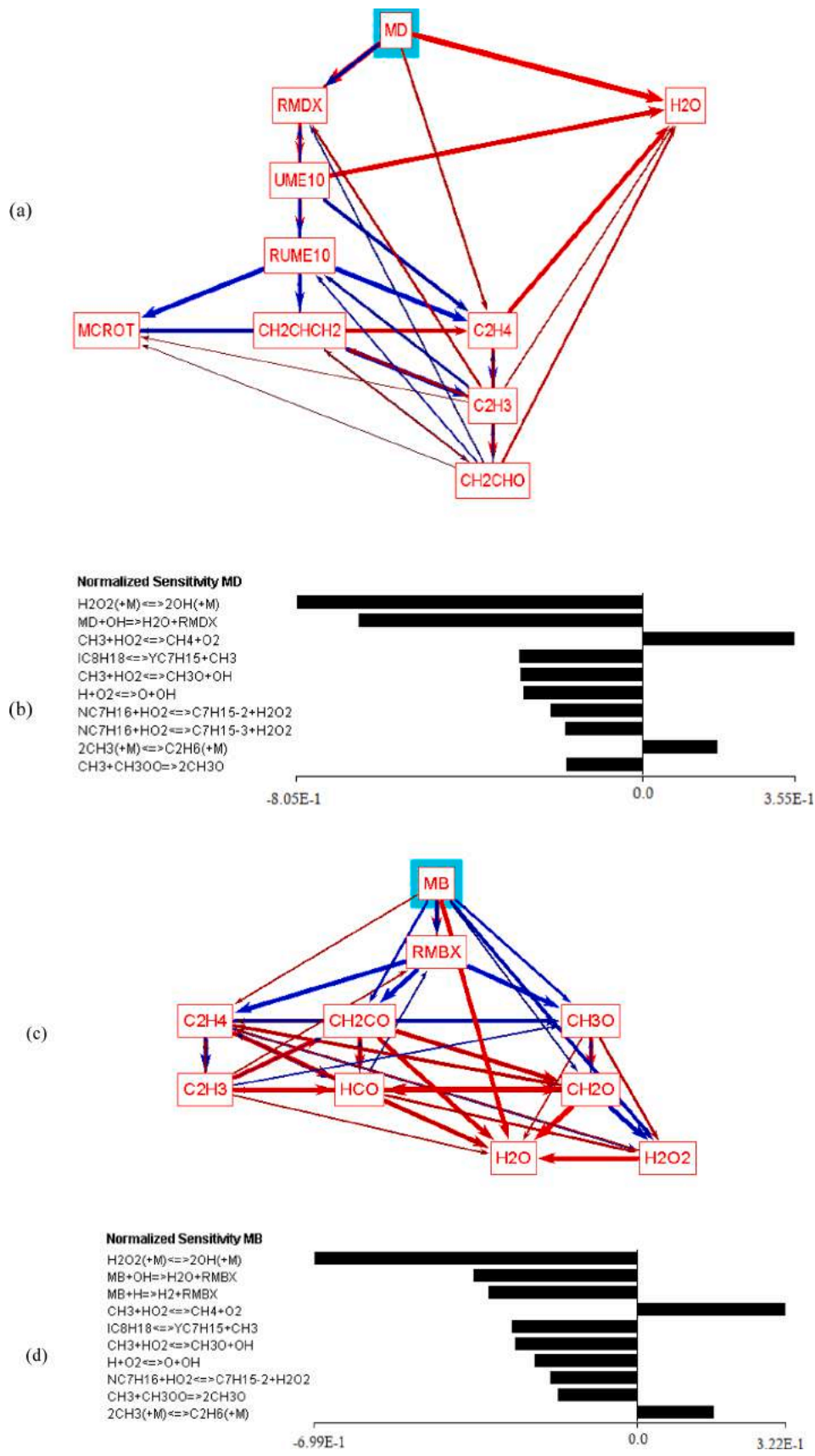


Fig. 5. Normalised combustion sensitivity and reaction path analysis of MB and MD.

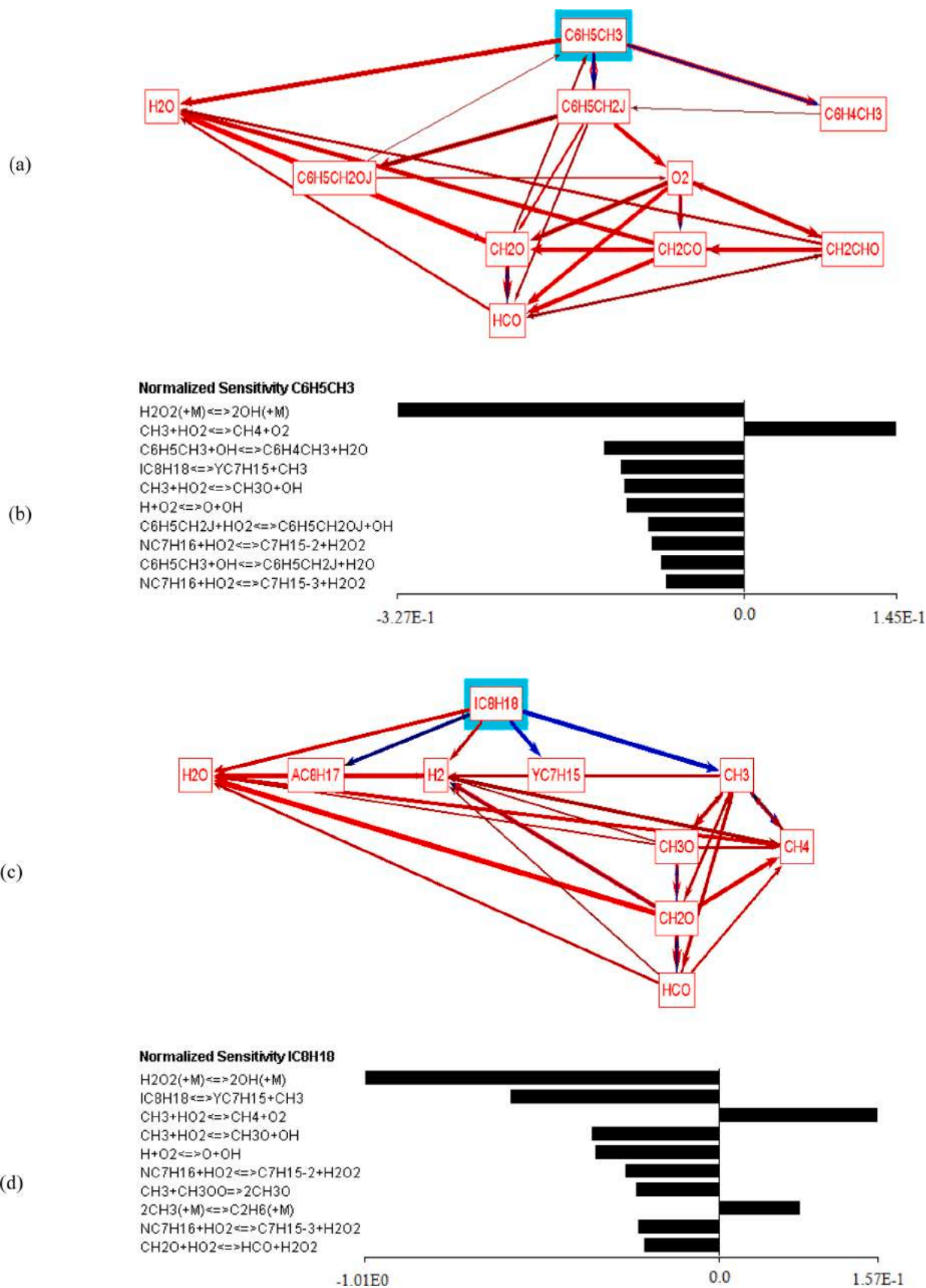


Fig. 6. Normalised combustion sensitivity and reaction path analysis of toluene and isoctane.

Table 1
The identified cross-reactions.

Reactions		A (s ⁻¹)	B	E _a (J/mol)
NC7H16+C7H15O2-1<=>C7H15-3+C7H15O2H-1		8.064E+12	0.00	1.770E+04
	Rev	1.440E+10	0.00	1.500E+04
NC7H16+C7H15O2-2<=>C7H15-3+C7H15O2H-2		8.064E+12	0.00	1.770E+04
	Rev	1.440E+10	0.00	1.500E+04
NC7H16+C7H15O2-3<=>C7H15-3+C7H15O2H-3		8.064E+12	0.00	1.770E+04
	Rev	1.440E+10	0.00	1.500E+04
NC7H16+C7H15O2-4<=>C7H15-3+C7H15O2H-4		8.064E+12	0.00	1.770E+04
	Rev	1.440E+10	0.00	1.500E+04
AC8H17O2 + NC7H16 = AC8H17O2H + C7H15-3		8.06E+12	0	17,700
BC8H17O2 + NC7H16 = BC8H17O2H + C7H15-3		8.06E+12	0	17,700
CC8H17O2 + NC7H16 = CC8H17O2H + C7H15-3		8.06E+12	0	17,700
DC8H17O2 + NC7H16 = DC8H17O2H + C7H15-3		8.06E+12	0	17,700
C7H15 - 3 + C6H12-1 = NC7H16 + C6H111-3		7.000E+10	0.00	8.900E+03
C7H15 - 3 + C6H12-1 = NC7H16 + C6H111-4		5.000E+10	0.00	1.140E+04
C7H15 - 3 + C6H12-1 = NC7H16 + C6H111-5		5.000E+10	0.00	1.140E+04
C7H15 - 3 + C6H12-1 = NC7H16 + C6H111-6		5.000E+10	0.00	1.440E+04
C7H15 - 3 + C2H5OH = NC7H16 + PC2H4OH		5.000E+10	0.00	1.440E+04
C7H15 - 3 + C2H5OH = NC7H16 + SC2H4OH		7.000E+10	0.00	8.900E+03
NC7H16 + C7H15O2-1<=>C7H15-2+C7H15O2H-1		8.064E+12	0.00	1.770E+04
	Rev	1.440E+10	0.00	1.500E+04
NC7H16 + C7H15O2-2<=>C7H15-2+C7H15O2H-2		8.064E+12	0.00	1.770E+04
	Rev	1.440E+10	0.00	1.500E+04
NC7H16 + C7H15O2-3<=>C7H15-2+C7H15O2H-3		8.064E+12	0.00	1.770E+04
	Rev	1.440E+10	0.00	1.500E+04
NC7H16 + C7H15O2-4<=>C7H15-2+C7H15O2H-4		8.064E+12	0.00	1.770E+04
	Rev	1.440E+10	0.00	1.500E+04
AC8H17O2 + NC7H16 = AC8H17O2H + C7H15-2		8.06E+12	0	17,700
BC8H17O2 + NC7H16 = BC8H17O2H + C7H15-2		8.06E+12	0	17,700
CC8H17O2 + NC7H16 = AC8H17O2H + C7H15-2		8.06E+12	0	17,700
DC8H17O2 + NC7H16 = AC8H17O2H + C7H15-2		8.06E+12	0	17,700
C7H15-2 + C6H12-1 = NC7H16 + C6H111-3		7.000E+10	0.00	8.900E+03
C7H15-2 + C6H12-1 = NC7H16 + C6H111-4		5.000E+10	0.00	1.140E+04
C7H15-2 + C6H12-1 = NC7H16 + C6H111-5		5.000E+10	0.00	1.140E+04
C7H15-2 + C6H12-1 = NC7H16 + C6H111-6		5.000E+10	0.00	1.440E+04
C7H15-2 + C2H5OH = NC7H16 + PC2H4OH		5.000E+10	0.00	1.440E+04
C7H15-2 + C2H5OH = NC7H16 + SC2H4OH		7.000E+10	0.00	8.900E+03
IC8H18 + NC7H15 = NEOC7H16 + AC8H17		1.500E+11	0.00	1.340E+04
IC8H18 +YC7H15 = C7H16-24 + AC8H17		1.500E+11	0.00	1.440E+04
IC8H18 +YC7H15 = C7H16-24 + BC8H17		5.000E+10	0.00	1.140E+04
IC8H18 +YC7H15 = C7H16-24 + CC8H17		1.000E+11	0.00	8.900E+03
IC8H18 +YC7H15 = C7H16-24 + DC8H17		1.000E+11	0.00	1.440E+04
C2H5+MD=>C2H6+RMDX		2.4000e+05	2.000	6700.00
C3H5-S+MD=>C3H6+RMDX		3.2400e+05	2.000	4500.00
C3H5-T+MD=>C3H6+RMDX		3.2400e+05	2.000	4500.00
C3H5-A+MD=>C3H6+RMDX		6.4680e+05	2.000	12,800.00
CH3O+MD=>CH3OH+RMDX		5.1360e+05	2.000	1500.00
CH2OH+MD=>CH3OH+RMDX		3.3960e+05	2.000	10,200.00
CH3O2+MD=>CH3O2H+RMDX		9.1200e+05	2.000	12,600.00
C2H5O2+MD=>C2H5O2H+RMDX		9.1200e+05	2.000	12,600.00
NC3H7O2+MD=>C3H7OOH+RMDX		9.1200e+05	2.000	12,600.00
CH3C6H4+MD=>C7H8+RMDX		4.4400e+08	1.000	2000.00
C2H5+MB=>C2H6+RMBX		1.2000e+05	2.000	6700.00
C3H5-S+MB=>C3H6+RMBX		1.6200e+05	2.000	4500.00
C3H5-T+MB=>C3H6+RMBX		1.6200e+05	2.000	4500.00
C3H5-A+MB=>C3H6+RMBX		3.2340e+05	2.000	12,800.00
CH3O+MB=>CH3OH+RMBX		2.5680e+05	2.000	1500.00
CH2OH+MB=>CH3OH+RMBX		1.6980e+05	2.000	10,200.00
CH2CHO+MB=>CH3CHO+RMBX		1.3800e+05	2.000	11,500.00

PRO. One limitation faced throughout the modelling process concerns the RCM conditions since they involve substantial ID timings and consequently large heat loss effects. Hence, bearing in mind the uncertainties involved in the knowledge of the experimental conditions, the results presented here have been retrieved using an adiabatic model, and so some quantitative discrepancies could be expected under certain conditions [72]. Moreover, the CDBG sub-mechanisms were validated individually, which meant that the fuel volume fraction was defined as 1 for each fuel component each time.

3.1.1. Reduced kinetic mechanism of diesel

The ID timing of the detailed, reduced and CDBG sub-mechanism for n-heptane are given in Fig. 7. As shown, the NTC region has been

accurately replicated by either the detailed or the reduced mechanisms. However, it is worthy to mention that for $P = 10$ atm and $T = < 770$ K, the detailed mechanism underestimates the ID timings with an error of approximately 30%. While, as for the rest of the temperature ranges the error takes $E < 10\%$. Nevertheless, the detailed mechanism's predicted ID timings correspond well with the experimental data for the NTC temperature region with associated errors of 5% for low and high pressures for the entire applied temperature range. As for the prediction capabilities of the reduced and CDBG sub-mechanism, the overall trend of the experimental data, particularly as for the NTC region, has been well-reproduced. However, their prediction accuracy is compromised for $P = 10$ atm and $P = 20$ atm. To be more exact, there is a shift to the left for the reduced and CDBG sub-mechanism, which makes their ID timing to

Table 2

Identified reactions for Arrhenius rate constants' optimization with their corresponding adjusted Arrhenius rate constants.

Reactions		Original Arrhenius rate constants			Adjusted Arrhenius rate constants		
		A (s^{-1})	b	E_a ($J.mol^{-1}$)	A (s^{-1})	b	E_a ($J.mol^{-1}$)
n-heptane							
NC7H16+HO2<=>C7H15-2 + H2O2	Rev*	1.264E2	3.37	1.372E4	1.05E2	3.37	1.372E4
		4.982E-1	3.66E0	2.562E3	4.982E-1	3.66E0	2.562E3
NC7H16+HO2<=>C7H15-3 + H2O2		1.264E2	3.37	1.372E4	1.05E2	3.37	1.372E4
	Rev	4.982E-1	3.66E0	2.562E3	4.982E-1	3.66E0	2.562E3
NC7H16+OH<=>C7H15-1 + H2O		2.57E7	1.8	9.54E2	0.11E7	1.8	9.54E2
	Rev	2.952E4	2.33E0	1.818E4	2.952E4	2.33E0	1.818E4
NC7H16+OH<=>C7H15-2 + H2O		4.9E6	2.0	-5.96E2	1.5E6	2.0	-5.96E2
	Rev	3.624E2	2.87E0	1.914E4	3.624E2	2.87E0	1.914E4
NC7H16+OH<=>C7H15-3 + H2O		4.9E6	2.0	-5.96E2	1.5E6	2.0	-5.96E2
	Rev	3.624E2	2.87E0	1.914E4	3.624E2	2.87E0	1.914E4
NC7H16+OH<=>C7H15-4 + H2O		2.45E6	2.0	-5.96E2	0.25E6	2.0	-5.96E2
	Rev	3.61E2	2.87E0	1.914E4	3.61E2	2.87E0	1.914E4
MB							
MB+OH=H2O+RMBX		2.396E6	2.0	-2.25983E3	0.752E6	2.0	-2.25983E3
MD							
MD+OH=H2O+RMDX		4.793E6	2.0	-2.25983E3	2.21E6	2.0	-2.25983E3
Iso-octane							
IC8H18<=>YC7H15+CH3		1.635E27	-2.794	8.393E4	1.428E27	-2.794	8.393E4
	Rev	1.63E13	0.0E0	-5.96E2	1.63E13	0.0E0	-5.96E2
Toluene							
C6H5CH3+OH=C6H5CH2J+H2O		1.77E5	2.394	-6.018E2	1.45E5	2.394	-6.018E2
C6H5CH2J+HO2=C6H5CH2OJ+OH		5.0E12	0.0	0.0E0	4.48E12	0.0	0.0E0

* Rev stands for reversible reactions.

Table 3

The corresponding operating conditions of the experimental data for each fuel.

CDBG component	Operating conditions		Equivalence ratio (Φ)	References
	Pressure	Temperature		
Diesel ^a	10, 20, 41 atm	600–1100 K	1	[35, 40, 41]
Biodiesel ^a	1, 4, 16 atm	600–1700 K	0.25, 0.5, 1, 1.5	[73, 74]
Gasoline ^b	50 bar	600–1100 K	0.3, 0.5	[55, 75]

^a Experimental data under ST conditions.^b Experimental data under RCM conditions.^c Φ =(actual fuel/air ratio)/(stoichiometric fuel/air ratio).

carry erroneous values of up to 45%, at $P = 10$ and $P = 20$ atm within the temperature range of 770–900 K. This shift in the ID timing trend line is caused mainly by the elimination of some reactions, and consequently their pre-exponential factor, which were important to form analogous line pattern [1]. Thus, as a result of omitting those accountable reactions the ID values are either overestimated or underestimated for particular temperature ranges, which ultimately causes the trend line to shift from the base line. Contrarily, by increasing the pressure to $P = 40$ atm, the reduced and CDBG sub-mechanism revealed more accurate ID predictions and the associated shift in trend line tends to fade away.

3.1.2. Reduced kinetic mechanism of biodiesel

The results of the detailed, reduced and CDBG sub-mechanism for the biodiesel surrogate (MB and MD) have been compared to the experimental data in Fig. 8. As shown in Fig. 8-a&b, the detailed MD mechanism accurately predicted the NTC region as well as the ID timing's overall trend line compared to the experimental data, however, for higher equivalence ratios and temperatures, a slight shift to the left in the ID timing trend is detected. The highest error associated with the detailed mechanism has been perceived for $\Phi=1.5$ and $T=>952$ K with error of 30%, which in some cases reaches 40% as the worst case. Nonetheless, as the fuel per air ratio decreases to stoichiometric condition ($\Phi=1$), the detailed mechanism portrays significantly lower errors, as such error of 10–18% has been identified for $T = 952$ –1111 K. Furthermore, the reduction in equivalence ratio to fuel-lean conditions ($\Phi=0.5$) has improved the ID timing emulation of the detailed

mechanisms and the downsides of $T = 952$ –1111 K has been altered.

On the other hand, the reduced MD mechanism has revealed analogous trend pattern compared with experimental data, however, some errors are observed. As such, at $\Phi=1.5$ the ID values have been underestimated for the NTC region with error of 40%, which reaches up to over 55% in the vicinity of $T = 870$ K. Also, it is overestimated sharply at temperatures above 930 K with noticeably high error of 55% which increases up to 60% as the temperature rises. On the contrary, as for the lower Φ values the reduced mechanism tends to reproduce more accurate results. However, the ID timing at the vicinity of NTC region is still concerned because the errors can get as high as 57% (for $\Phi=1$). Additionally, the best results have been achieved for $\Phi=0.5$ with lowest error of 2% at $T=$ around 800 K and the highest error of 29% at $T = 1052$ –1070 K. Moreover, in the case of the CDBG sub-mechanism of MD, similar pattern to the reduced mechanism has been found with one difference at the vicinity of the NTC region; to be more exact, the ID timing in this region has been further compromised that improves by the decrease in the Φ value.

On the other hand, Fig. 8-c&d portrays the ID timing results of MB mechanisms. Although the general ID trend for $\Phi=1$ has been accurately replicated by the detailed and reduced mechanisms, there is still a huge difference between the predicted ID values with experimental data. To be more precise, there is a constant error of 42% that is retained throughout the whole temperature range with no sign of improvement by the increase in pressure to 4 atm. Similar difference in ID timing of CDBG sub-mechanism and experimental data has also been found for this operating condition. Contrarily, in the case of $\Phi=0.25$ all the detailed, reduced, and CDBG sub-mechanism illustrate perfect correspondence with experimental data for the entire applied operating conditions. In other words, the associated error has been retained at <8%, with only an exception in $T = 1430$ K and $P = 4$ atm with error of 16%.

3.1.3. Reduced kinetic mechanism of gasoline

Fig. 9 provides the predicated ID timings of the gasoline surrogate (toluene & iso-octane). Firstly, it must be highlighted that the NTC regions in both diagrams has been well-replicated. However, the ID values of detailed mechanism is lower than experimental data so as the reduced and CDBG sub-mechanisms for $\Phi=0.3$ and $T = 715$ –833 K with fluctuating errors of 35–55%. Nonetheless, in the case of $\Phi=0.5$ there is a

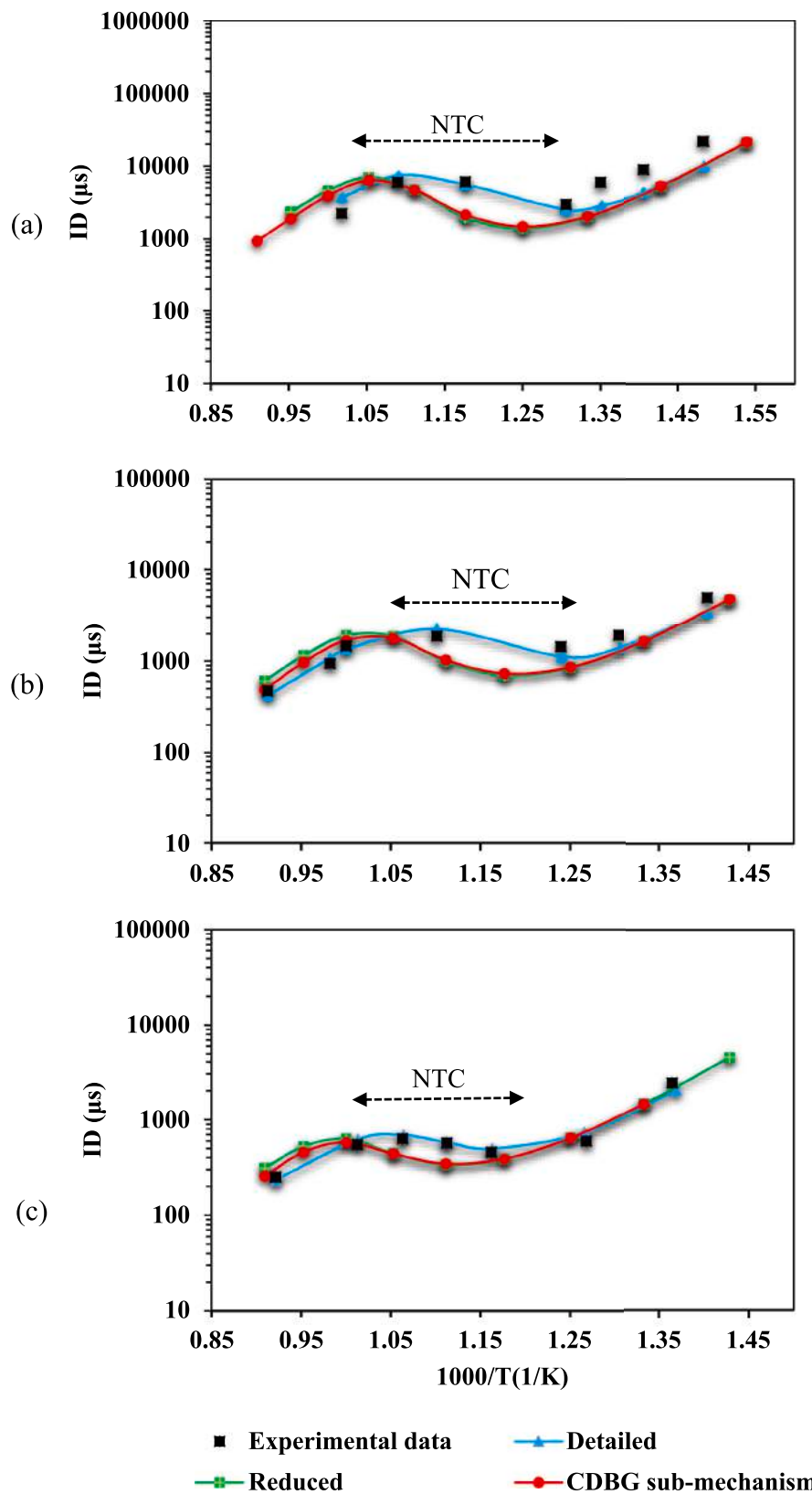


Fig. 7. The comparison of detailed, reduced, and CDBG sub-mechanism of n-heptane with experimental data at (a) 10 atm, (b) 20 atm, and (c) 41 atm [35, 40, 41].

noticeable increase in the emulating abilities of all the mechanisms. As such, only high errors have been discerned in the vicinity of $T = 800$ K, whilst, as for other temperature regions the detailed and reduced mechanisms presented acceptable ID timings with $E < 10\%$. To be more

exact, at for $\Phi = 0.5$ the detailed and reduced mechanisms have marginally higher and lower ID values compared to the experimental data, respectively while the CDBG sub-mechanism showed the best predicted ID values for the entire given temperature.

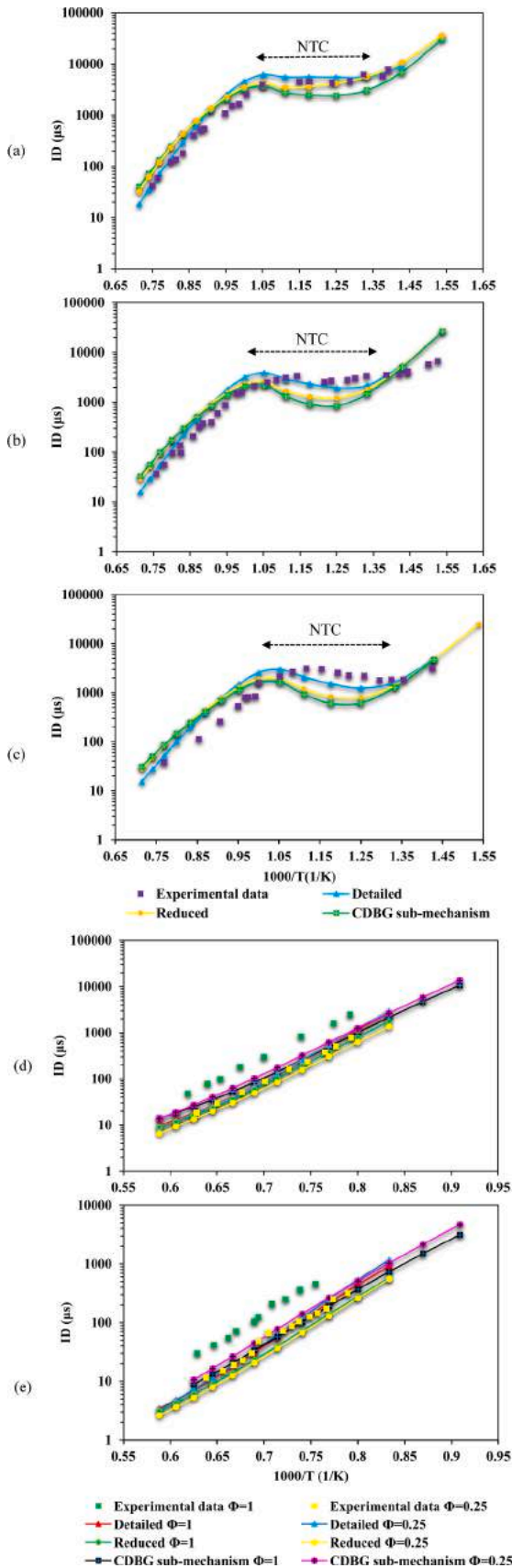


Fig. 8. The comparison of detailed, reduced, and CDBG sub-mechanism with experimental data [48, 74] for MD at equivalence ratios of (a) 0.5, (b) 1, and (c) 1.5 and MB at pressures of (d) 1 atm and (e) 4 atm.

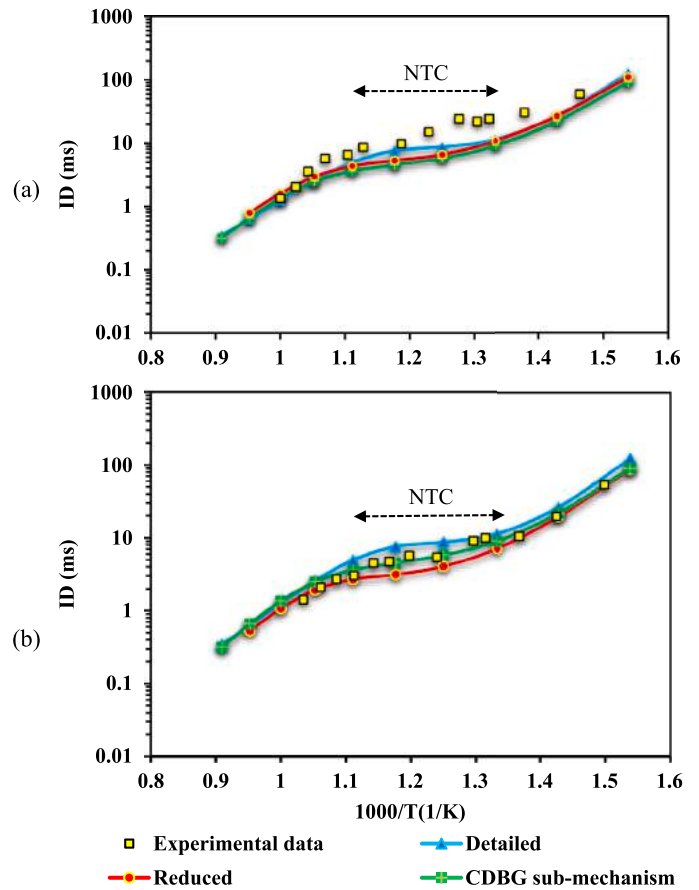


Fig. 9. The comparison of detailed, reduced, and CDBG sub-mechanism of isooctane & toluene with experimental data at equivalence ratios of (a) 0.3 and (b) 0.5 [40, 55].

3.2. The effects of cross-reactions and Arrhenius rate constant optimisation on the ignition delay timing

To analyse the effects of integrating the cross-reactions and Arrhenius rate constants optimisation methods on the ID prediction, the ID timings predicted by each analysis are compared with experimental data using the relative difference of their ID values as follows:

$$Error (\%) = \frac{ID_{new\ CDBG} - ID_{Experimental\ data}}{ID_{Experimental\ data}} \times 100 \quad (10)$$

It must be noted that for simplification purposes, CR has been used as a short for cross-reaction and AR is used for Arrhenius rate optimisation throughout the plots presented in the next section. So, the results for three scenarios of pure CDBG mechanism, CDBG mechanism integrated with sole CR, and dual utilisation of CR and AR methods are presented in the following parts.

3.2.1. Diesel surrogate oxidation

Fig. 10 depicts the results of AR and CR approaches for CDBG sub-mechanism of n-heptane. According to the outcomes, the dual integration of CR and AR method revealed generally more accurate results compared to CR method in improving the ID timing, particularly for $P = 10$ atm and 20 atm. To begin with, the CR method has caused a slight enhancement for the ID timing at the NTC region compared to pure CDBG mechanism. Also, the integration of AR method has brought about significantly accurate predictions for $T = 750-900$ K, as such the associated error takes maximum 15% and minimum 3.2% for $P = 10$ atm and 20 atm. Nonetheless, at $P = 41$ atm both CR and AR methods deviate slightly from the experimental data with maximum errors of 14.654%

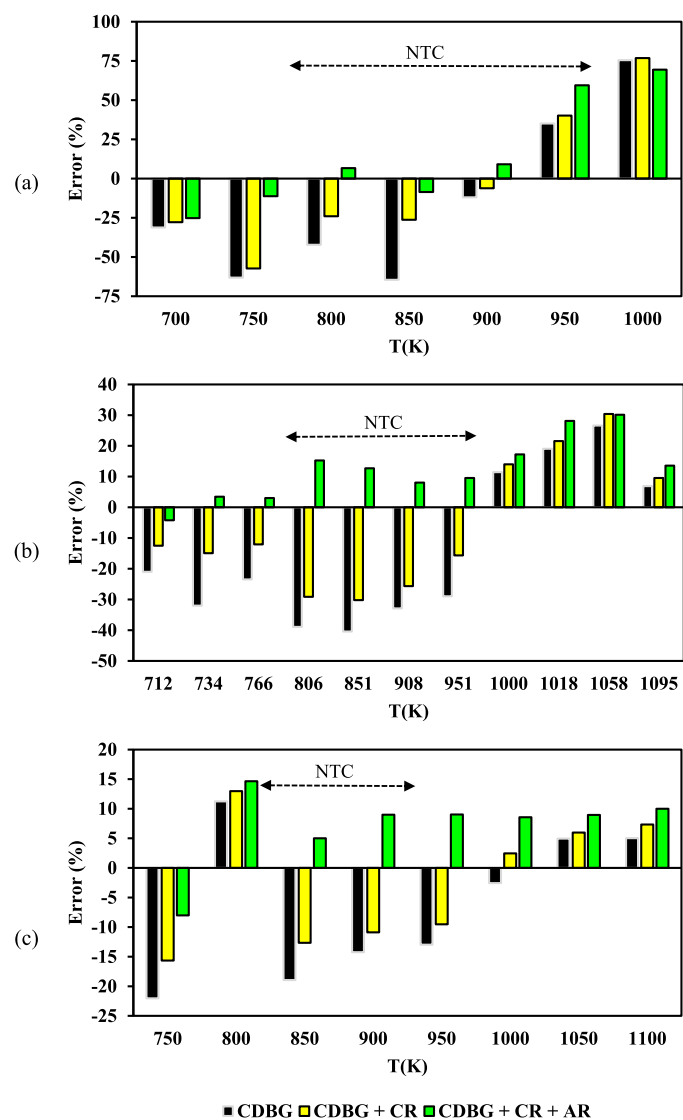


Fig. 10. The associated ID timing errors for CDBG sub-mechanism of n-heptane with CR and AR adjustment compared to experimental data at (a) 10 atm, (b) 20 atm, and (c) 41 atm.

(at $T = 900$ K) and 15.6% (at $T = 750$ K), respectively. In addition, it can be discerned that for $P = 10$ atm and $T = 1000$ K the associated errors in both approaches reach higher values up to 69%. Lastly, in the case of $P = 41$ atm, the AR technique presented very accurate ID timings with almost 6% for more than 75% of the temperature range, whilst, for $T = 800$ K the trend was slightly overestimated (14.5%). Contrarily, the implementation of the CR method has performed more accurately compared to dual CR and AR methods for $T = 800$ K and $T \geq 950$ K. In conclusion, the best performance for dual integration of CR and AR methods has been ascertained for $P = 40$ atm (all the temperature range), followed by $P = 20$ atm ($T < 1000$ K) and $P = 10$ atm ($T < 950$ K).

3.2.2. Biodiesel surrogate oxidation

The ID profiles for the applied AR and CR methods on the CDBG sub-mechanisms of MD and MB are illustrated in Fig. 11. To begin with, as for the MD case, the CR method has revealed noticeable adjustments compared to pure CDBG mechanism, particularly for the NTC region and $\Phi = 0.5$. Also, the dual integration of CR and AR methods has offered significantly more accurate results compared to the sole CR method for all the operating conditions. Also, there is a noticeable improvement for

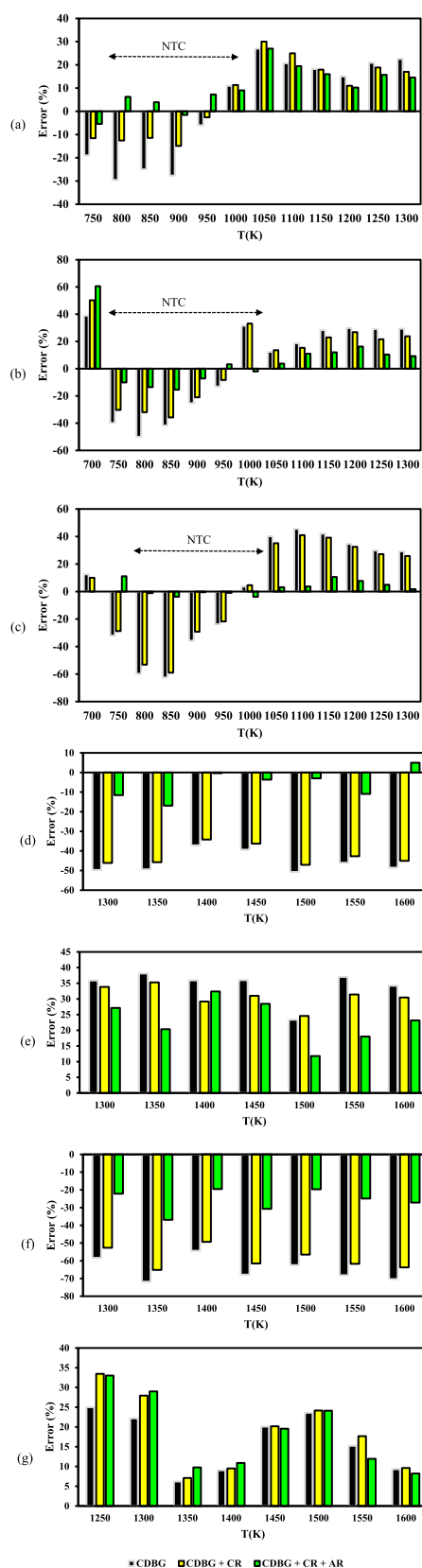


Fig. 11. The associated ID timing errors for CDBG sub-mechanism with CR and AR adjustment compared to experimental data for MD at equivalence ratios of (a) 0.5, (b) 1, and (c) 1.5 and MB at (d) $P = 1$ atm and $\Phi = 1$, (e) $P = 1$ atm and $\Phi = 0.25$, (f) $P = 4$ atm and $\Phi = 1$, (g) $P = 4$ atm and $\Phi = 0.25$.

the MD's ID predictions for the case of AR and CR dual integration, particularly as for $\Phi=1.5$. As such, the associated errors have not reached above 11.8% throughout the applied temperature range. Furthermore, the addition of AR method for $\Phi=0.5$ and 1 has resulted in substantially lower errors in replicating the ID timing; as such, for the NTC region the error fluctuates between -1.5% (negative sign for underestimation) and 15% , with just a slight overestimation for $T > 1111$ K that caused the error to reach 27% and 16% for $\Phi=0.5$ and 1, respectively. Concisely, the dual integration of CR and AR methods provides the best predictions of MD's ID timing for $\Phi=1.5$, followed by $\Phi=1$ ($T > 750$ K) and $\Phi=0.5$ ($T < 1050$ K).

Moreover, as for the CDBG sub-mechanism of MB, it can be inferred that the ID timing for both $P = 1$ atm and 4 atm has been improved for dual CR and AR methods incorporation at $\Phi=1$. In other words, the associated error is as low as -16% for this operating condition under the entire temperature range (at $P = 1$ atm). Furthermore, the CR method integration for $\Phi=1$ has resulted marginal improvements, as such, the error still fluctuates between 40% and 55% . Also, the increase in pressure from 1 atm to 4 atm leads the CR method to compromise the accuracy of the ID timing and slight increase in errors is perceived. Similarly, the addition of AR method is found to increase the errors slightly for $P = 4$ atm and $\Phi=0.25$. In summary, the dual integration of CR and AR for the ID timing of MB provides accurate results for $P = 1$, 4 atm and $\Phi=1$.

3.2.3. Gasoline surrogate oxidation

The results of ID timing profile for the CDBG sub-mechanism of gasoline surrogates are shown in Fig. 12. First, the integration of CR method has slightly improved the ID timing compared to pure CDBG mechanism particularly for $\Phi=0.3$. Also, the AR method has provided more precise results compared to CR method especially for $\Phi=0.3$. Better agreement between the dual CR and AR incorporation with the experimental data has been achieved for $\Phi=0.3$ with associated error of

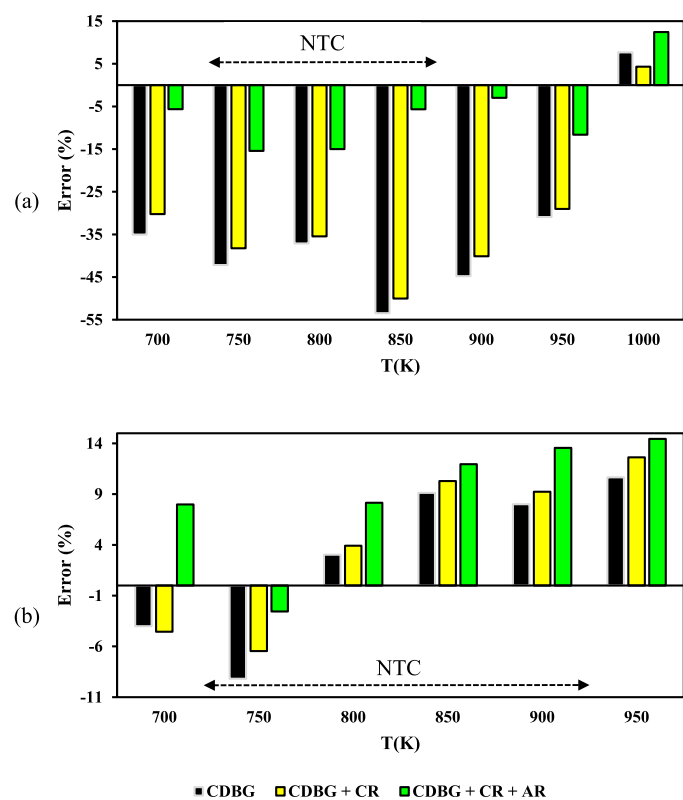


Fig. 12. The associated ID timing errors for CDBG sub-mechanism with CR and AR adjustment compared to experimental data for toluene and isooctane at equivalence ratios of (a) 0.3 and (b) 0.5.

less than 15% for the entire given temperature range. Conversely, in the case of $\Phi=0.5$, the pure CDBG mechanism already agrees well with the experimental data, and the applied methodologies have been able to improve the ID timing only at $T = 750$ K. Finally, the dual utilisation of CR and AR methods gives accurate ID predictions for $\Phi=0.3$, followed by $\Phi=0.5$ ($T = 750$ K).

3.3. Validations of flame speed and species mole fractions

As far as the robustness of kinetic mechanisms is concerned, it is imperative to ascertain their replicating abilities in terms of other important benchmarks such as flame speed and species mole fractions. Henceforth, in the present study it is also attempted to validate the proposed CDBG mechanism regarding the abovementioned criteria. It must be noted that the results provided in the following sections are just for the final CDBG mechanism that has been equipped with the results obtained for dual integration of the CR and AR methods. Furthermore, due to the lack of adequate experimental data, the detailed mechanisms have been used as the main benchmarking target for comparing the flame speed of n-heptane and species' mole fraction of isooctane & toluene.

3.3.1. CDBG sub-mechanism of diesel

The results of flame speed and species' mole fraction for CDBG sub-mechanism of n-heptane has been given in Fig. 13. From now on, when CDBG mechanism is mentioned, pure CDBG is not intended but the CDBG mechanism that has been altered with CR and AR techniques

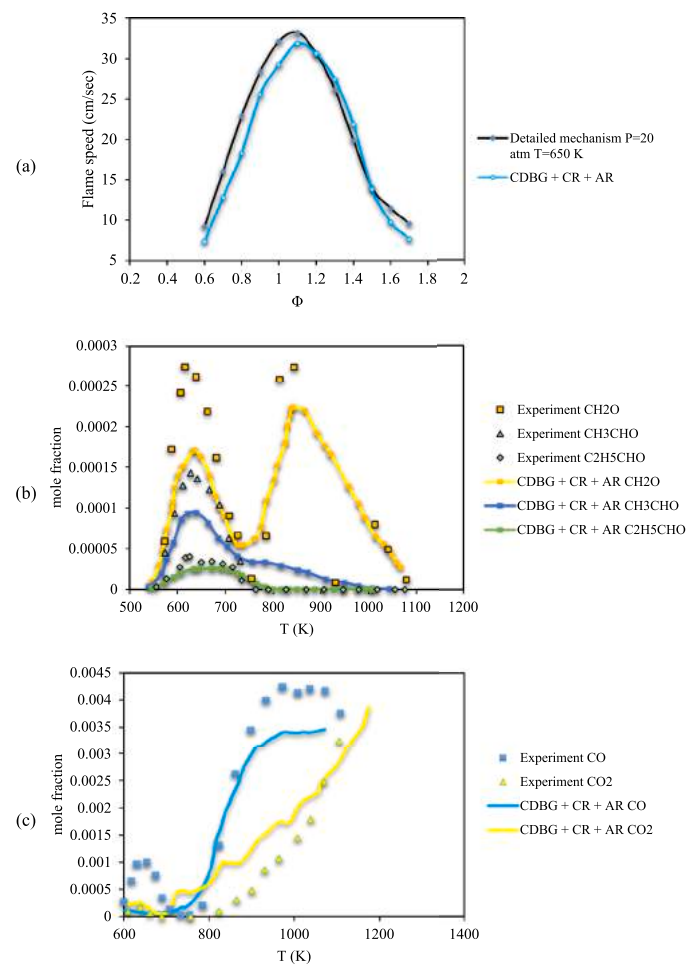


Fig. 13. The flame speed species' mole fraction of CDBG sub-mechanism of n-heptane and corresponding experimental data at $P = 10$ atm and $\Phi=1$ [35, 76, 77].

(final proposed mechanism). To begin with, as it is given in Fig. 13-a, the flame speed of the detailed mechanism has been well-replicated by the CDBG mechanism. As such, the associated errors reach maximum 6% throughout the entire given equivalence ratio range. Furthermore, as for the species' mole fractions, the Fig. 13-b&c portrays a precise correspondence of the CDBG mechanism with the experimental data; in fact, the highest associated error is recognized for CH₂O and CO with maximum error of 18% (at the vicinity of $T = 800$ K and 900 K) and 17% (at the vicinity of $T = 850$ –1150 K), while, the results for other temperature ranges has been in good agreements with experimental data with $E < 10\%$.

3.3.2. CDBG sub-mechanism of biodiesel

Fig. 14 depicts the flame speed and species' mole fraction for CDBG mechanism of MD and MB. Firstly, in the case of flame speed both CDBG sub-mechanisms of MD and MB has performed accurate enough, with a slight shift to the right for the case of MB at $P = 1$ atm and $T = 403$ K. To be more exact, the flame speeds of MD and MB have been well-emulated by the CDBG mechanism with error of $E < 5\%$ and $E < 2\%$, respectively, except for MB case at $P = 1$ atm, $T = 403$ K and $\Phi > 1$ with maximum 12% of error. Moreover, as it can be perceived from the predictions the species' mole fractions have been precisely imitated with associated errors of $E < 6\%$ for the entire applied temperature range.

3.3.3. CDBG sub-mechanism of gasoline

The results of flame speed and species' mole fraction for the CDBG sub-mechanism of isooctane & toluene have been illustrated in Fig. 15. Comparing the predicted flame speeds, it can be noticed that CDBG mechanism has adequately mimicked the experimental data with errors of $E < 8\%$. In addition, the prediction of species' mole fraction is also in good agreement with the experimental data, as such, the detected error has been kept within $E < 8\%$, with an exception for CO, CH₂O, and CH₄ which error of $E \approx 20\%$ for $T = 1100$ –1500 K is perceived.

3.4. Comparison of runtimes for the mechanisms

As declared before, one of the important ideas that lie behind the seek for reducing kinetic mechanisms is to introduce manageable mechanisms that can be feasibly incorporated in 3-D simulations. Although the detailed mechanisms can provide accurate predictions of combustion-related characteristics, yet again, their associated runtime is hugely impractical. Thus, it is also attempted to analyse the differences between the required runtimes of detailed and reduced mechanisms under analogous setups as described in the previous section. The utilised computer's specifications are as follows: CPU E5-2660 v3 @ 2.60 GHz, RAM 64 GB, with 10 parallel processors for each run throughout the CHEMKIN-PRO simulations. The results of the detailed and reduced mechanisms' runtimes for each fuel surrogate in conjunction with their corresponding number of setups are presented in Fig. 16. The integrated detailed mechanisms of biodiesel surrogates (MD & MB) revealed an average runtime of 36 min, followed by 21 min and 10 min for the gasoline and diesel surrogates, respectively. Conversely, the reduced mechanisms performed the simulations within a considerably lower duration of time for the similar applied setups; as such, averages of 8 min, 5 min and 3 min for the biodiesel, gasoline and diesel surrogates, respectively was required to finish the modelling. In other words, the runtime has been reduced by 70%, 78% and 76% for biodiesel, diesel and gasoline surrogates, respectively.

It is also worthy to mention that since gasoline surrogate mechanism had relatively higher mechanism size, it was expected to take more runtime to perform the tasks. However, the biodiesel surrogate mechanism had relatively more setups, as many as double of gasoline case to be exact. While this is deemed as the main accountable reason, bearing in mind the complexities associated with the detailed mechanisms, it is plausible to hypothesize that biodiesel mechanism had more associated reactions to go through (for the given setups) to finish the tasks. Last but

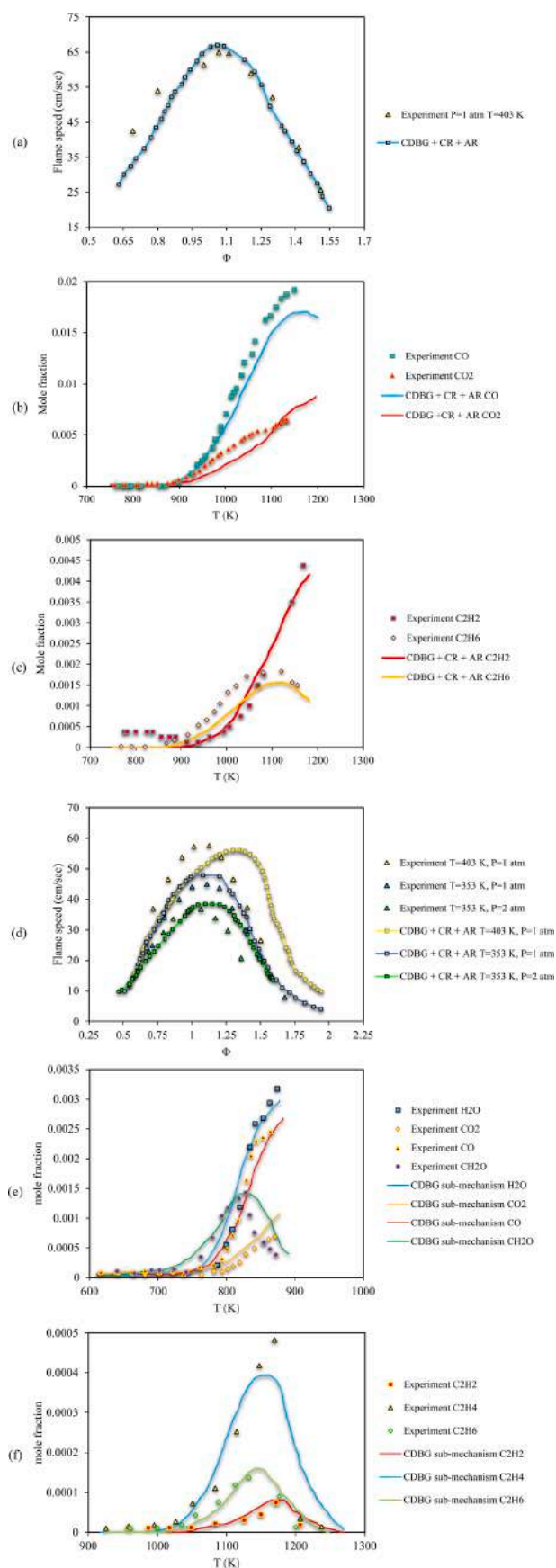


Fig. 14. The flame speed and species' mole fraction of CDBG sub-mechanism (a, b, c): of MD and their corresponding experimental data [74], and (d, e, f): MB with their corresponding experimental data [73].

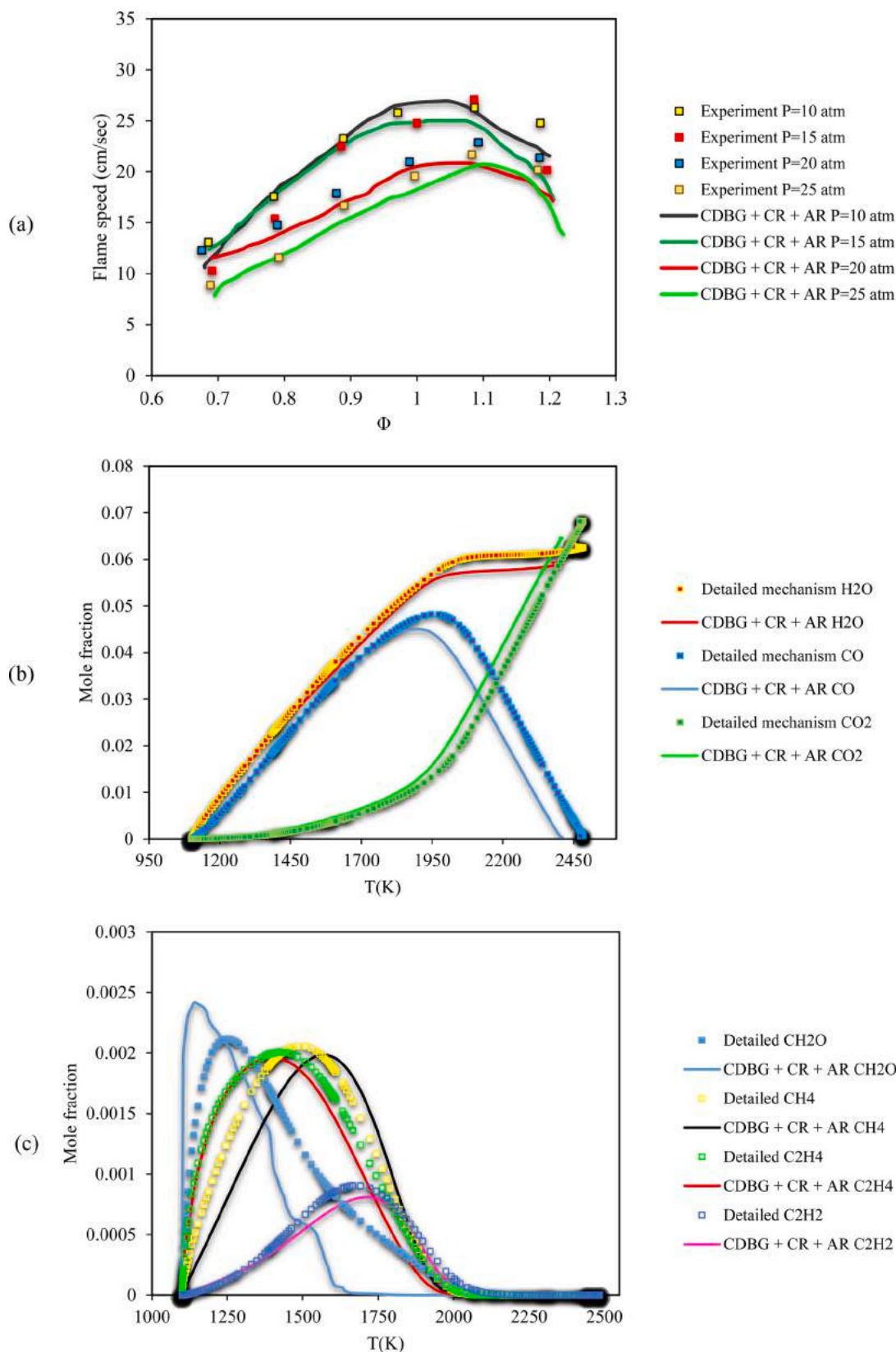


Fig. 15. The flame speed and species' mole fraction of CDBG sub-mechanism of isoctane & toluene and their corresponding experimental data [40, 54].

not least, to the best of the authors knowledge, since a high-performance computer is utilised (10 parallel processors) the difference between the required runtime for detailed and reduced mechanisms were not as noticeable as expected; while, this difference is expected to rise upon

considering more simulations setups.

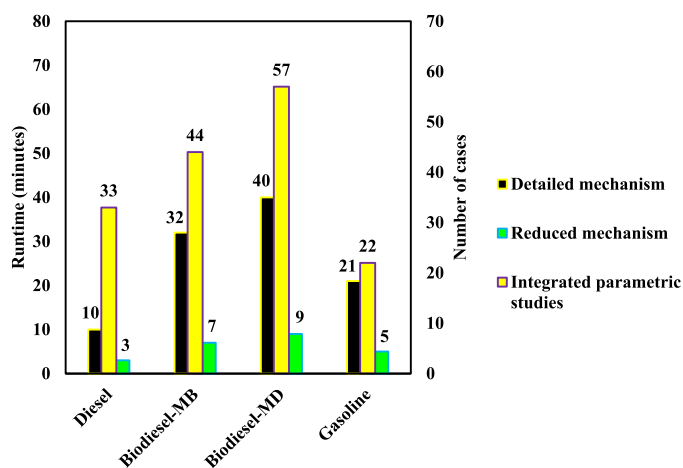


Fig. 16. The associated runtimes of detailed and reduced mechanisms for each fuel surrogate and their corresponding number of setups.

4. Conclusions

A compact reduced kinetic mechanism is developed to numerically characterise the ignition-related characteristics of diesel-biodiesel-gasoline mixtures. The DRG, DRGEP and FSSA mechanism reduction approaches are applied coupled with the cross-reactions analysis and the Arrhenius reaction rate constants optimisation method. The validation results revealed that the reduced mechanisms equipped with the cross-reactions and Arrhenius parameters optimisation were capable of accurately replicating the ID timing compared to the detailed reaction mechanism and the experimental data for a wide range of temperatures, pressures and equivalence ratios. In addition, the proposed multi-component CDBG mechanism best reproduced the measured ID timing, flame speed and species mole fraction at $T = 600\text{--}1700\text{ K}$ for $P = 41\text{ atm}$ and $\Phi = 1$, $P = 1,4\text{ atm}$ and $\Phi = 1$, and $P = 50\text{ bar}$ and $\Phi = 0.3$ with the maximum errors within 14.6%, 16.9% and 14.9% margins compared to the reference cases of diesel, biodiesel and gasoline, respectively.

Moreover, the effect of integrating cross-reactions technique is found to be more pronounced at low to medium temperatures for all the utilised surrogates. Also, the effect of cross-reactions is controlled by both the initial pressure and equivalence ratio; as such, the increase in the initial pressure and equivalence ratio boosts the influences of cross-reactions (except for MD mechanism), particularly for lower temperatures. Besides, the dual integration of cross-reaction and Arrhenius rate constants optimisation revealed higher improvement for the respective range except for the CDBG sub-mechanism of gasoline under high temperature and equivalence ratio where a maximum error of 14% was discerned.

Given the overall low reactivity level of the integrated fuels at low temperatures, incorporating the cross-reactions contributes to the enhanced interactions between the fuel components and promotes the formation of intermediate and small active molecules, which ultimately accelerates the reactions associated with the active components and reduces the ID timing. The same phenomena were discerned for the dual integration of cross-reaction and Arrhenius rate constants optimisation techniques. Nonetheless, with increased temperatures, the reaction rate associated with the elementary components is dramatically increased, and the utilisation of the proposed approaches did not noticeably increase the intermediate products' reaction rate. Therefore, the controlling effects of cross-reaction and Arrhenius rate constants optimisation techniques are limited. Lastly, significant reductions in the runtimes of up to 70%, 78% and 76% for biodiesel, diesel and gasoline surrogates, respectively were attained with the reduced mechanisms.

5. Limitations and recommendations for future work

One limitation faced in this research concerns the lack of experimental validation data for the combined mechanism of the ternary fuel mixture tested. Although the validity of all sub-mechanisms for each individual surrogate has been analysed in detail, it is worthy to highlight that a more reliable validation can be achieved once the presence of other fuels is also taken into account, both experimentally and numerically. Further experimental engine tests for the blends of diesel-biodiesel-gasoline are recommended to enhance the practical implementation of this newly introduced fuelling strategy.

The methodology applied in this investigation was to firstly reduce the mechanisms followed by merging. However, given the many possibilities associated with the reduction and merging stages, numerous mixture mechanisms are feasible to be generated. Furthermore, the accuracy of the final mechanism is dependant on the change in the approaches taken as discussed earlier. Given the time constraints of the project, not all possible combined mechanisms could be tested. As such, future investigations can look into reducing two mechanisms at a time for two fuels and merging the reduced mechanisms with the detailed mechanism of the third fuel, followed by reduction.

Another recommendation for future work is to consider selecting the reaction parameters for the detected mutual reactions of the master and donor mechanisms based on their influences on the reacting behaviour of the intended mechanism. In other words, it is crucial to choose the Arrhenius parameters for the identified commonalities according to their sensitivities towards combustion-related characteristics such as ID timing, flame speed and species mole fraction. To do so, the importance of the common reactions must first be ascertained and decisions for the Arrhenius rate constants of identified common reactions made thereafter according to their influential effects.

Declaration of Competing Interest

The authors declare that they have no known competing financial interests or personal relationships that could have appeared to influence the work reported in this paper.

Acknowledgements

The Ministry of Higher Education (MOHE), Malaysia is gratefully acknowledged for the financial support towards this project under the Fundamental Research Grant Scheme FRGS/1/2019/TK03/UNIM/01/1.

References

- [1] H.K. Ng, S. Gan, J.-H. Ng, K.M. Pang, Development and validation of a reduced combined biodiesel–diesel reaction mechanism, *Fuel* 104 (2013) 620–634.
- [2] E.M. Shahid, Y. Jamal, A review of biodiesel as vehicular fuel, *Renew. Sustain. Energy Rev.* 12 (9) (2008) 2484–2494.
- [3] A. Liaquat, H. Masjuki, M. Kalam, M. Fazal, A.F. Khan, H. Fayaz, M. Varman, Impact of palm biodiesel blend on injector deposit formation, *Appl. Energy* 111 (2013) 882–893.
- [4] X. Zhu, Ö. Andersson, Performance of new and aged injectors with and without fuel additives in a light duty diesel engine, *Transp. Eng.* 1 (2020), 100007.
- [5] M. Hoseinpour, H. Sadrmia, M. Tabasizadeh, B. Ghobadian, Energy and exergy analyses of a diesel engine fueled with diesel, biodiesel–diesel blend and gasoline fumigation, *Energy* 141 (2017) 2408–2420.
- [6] Y. Zhang, L. Zhan, Z. He, M. Jia, X. Leng, W. Zhong, Y. Qian, X. Lu, An investigation on gasoline compression ignition (GCI) combustion in a heavy-duty diesel engine using gasoline/hydrogenated catalytic biodiesel blends, *Appl. Therm. Eng.* 160 (2019), 113952. %@ 1359-4311.
- [7] F. Leach, G. Kalghatgi, R. Stone, P. Miles, The scope for improving the efficiency and environmental impact of internal combustion engines, *Transp. Eng.* 1 (2020), 100005.
- [8] M.S. Gad, M.A. Ismail, Effect of waste cooking oil biodiesel blending with gasoline and kerosene on diesel engine performance, emissions and combustion characteristics, *Process Saf. Environ. Prot.* 149 (2021) 1–10. %@ 0957-5820.
- [9] R. Hanson, D. Splitter, R.D. Reitz, Operating a heavy-duty direct-injection compression-ignition engine with gasoline for low emissions, *SAE Tech. Paper* (2009).

- [10] M. Sellnau, J. Sinnamon, K. Hoyer, H. Husted, Gasoline direct injection compression ignition (GDCI)-diesel-like efficiency with low CO₂ emissions, *SAE Int. J. Engines* 4 (1) (2011) 2010–2022.
- [11] M. Zandje, A. Kazemi, M. Ahmadi, M.K. Moraveji, A CFD investigation into the enhancement of down-hole de-oiling hydro cyclone performance, *J. Pet. Sci. Technol.* 199 (2021), 108352.
- [12] W.J. Pitz, C.J. Mueller, Recent progress in the development of diesel surrogate fuels, *Prog. Energy Combust. Sci.* 37 (3) (2011) 330–350.
- [13] M. Baratta, S. Chiriches, P. Goel, D. Misul, CFD modelling of natural gas combustion in IC engines under different EGR dilution and H₂-doping conditions, *Transp. Eng.* 2 (2020), 100018.
- [14] A. Bianco, F. Millo, A. Piano, Modelling of combustion and knock onset risk in a high-performance turbulent jet ignition engine, *Transp. Eng.* 2 (2020), 100037.
- [15] X. Cheng, Development of Reduced Reaction Kinetics and Fuel Physical Properties Models For In-Cylinder Simulation of Biodiesel Combustion, University of Nottingham, 2016.
- [16] X. Cheng, H.K. Ng, S. Gan, J.H. Ho, Advances in computational fluid dynamics (CFD) modeling of in-cylinder biodiesel combustion, *Energy Fuels* 27 (8) (2013) 4489–4506.
- [17] T. Lu, C.K. Law, A directed relation graph method for mechanism reduction, *Proc. Combust. Inst.* 30 (1) (2005) 1333–1341.
- [18] T. Lu, C.K. Law, Linear time reduction of large kinetic mechanisms with directed relation graph: n-Heptane and iso-octane, *Combust. Flame* 144 (1–2) (2006) 24–36. %@ 0010-2180.
- [19] L. Liang, J.G. Stevens, J.T. Farrell, A dynamic adaptive chemistry scheme for reactive flow computations, *Proc. Combust. Inst.* 32 (1) (2009) 527–534.
- [20] L. Liang, J.G. Stevens, S. Raman, J.T. Farrell, The use of dynamic adaptive chemistry in combustion simulation of gasoline surrogate fuels, *Combust. Flame* 156 (7) (2009) 1493–1502.
- [21] P. Pepiot-Desjardins, H. Pitsch, An efficient error-propagation-based reduction method for large chemical kinetic mechanisms, *Combust. Flame* 154 (1–2) (2008) 67–81.
- [22] X. Zheng, T. Lu, C. Law, Experimental counterflow ignition temperatures and reaction mechanisms of 1, 3-butadiene, *Proc. Combust. Inst.* 31 (1) (2007) 367–375.
- [23] H. An, W. Yang, A. Maghbouli, J. Li, K. Chua, A skeletal mechanism for biodiesel blend surrogates combustion, *Energy Convers. Manage.* 81 (2014) 51–59.
- [24] D. Alviso, F. Krauch, R. Román, H. Maldonado, R.G. dos Santos, J.C. Rolón, N. Darabiha, Development of a diesel-biodiesel-ethanol combined chemical scheme and analysis of reactions pathways, *Fuel* 191 (2017) 411–426.
- [25] F. Zhao, W. Yang, W. Yu, H. Li, Y.Y. Sim, T. Liu, K.L. Tay, Numerical study of soot particles from low temperature combustion of engine fueled with diesel fuel and unsaturation biodiesel fuels, *Appl. Energy* 211 (2018) 187–193.
- [26] J. Li, W. Yang, H. An, D. Zhou, W. Yu, J. Wang, L. Li, Numerical investigation on the effect of reactivity gradient in an RCCI engine fueled with gasoline and diesel, *Energy Convers. Manage.* 92 (2015) 342–352.
- [27] S. Ren, S.L. Kokjohn, Z. Wang, H. Liu, B. Wang, J. Wang, A multi-component wide distillation fuel (covering gasoline, jet fuel and diesel fuel) mechanism for combustion and PAH prediction, *Fuel* 208 (2017) 447–468.
- [28] W. Zhong, N.M. Mahmoud, Q. Wang, Numerical study of spray combustion and soot emission of gasoline-biodiesel fuel under gasoline compression ignition-relevant conditions, *Fuel* 310 (2022), 122293.
- [29] Z. Liu, L. Yang, E. Song, J. Wang, A. Zare, T.A. Bodisco, R.J. Brown, Development of a reduced multi-component combustion mechanism for a diesel/natural gas dual fuel engine by cross-reaction analysis, *Fuel* 293 (2021), 120388.
- [30] H.M. Poon, K.M. Pang, H.K. Ng, S. Gan, J. Schramm, Development of multi-component diesel surrogate fuel models-Part II: validation of the integrated mechanisms in 0-D kinetic and 2-D CFD spray combustion simulations, *Fuel* 181 (2016) 120–130.
- [31] Q. Wang, C. Chen, Simulated kinetics and chemical and physical properties of a four-component diesel surrogate fuel, *Energy Fuels* 31 (12) (2017) 13190–13197.
- [32] E. Ranzi, A. Frassoldati, A. Stagni, M. Pelucchi, A. Cuoci, T. Faravelli, Reduced kinetic schemes of complex reaction systems: fossil and biomass-derived transportation fuels, *Int. J. Chem. Kinet.* 46 (9) (2014) 512–542.
- [33] G. Xiao, Y. Zhang, J. Lang, Kinetic modeling study of the ignition process of homogeneous charge compression ignition engine fueled with three-component diesel surrogate, *Ind. Eng. Chem. Res.* 52 (10) (2013) 3732–3741.
- [34] R. Lin, L.L. Tavlarides, Thermophysical properties needed for the development of the supercritical diesel combustion technology: evaluation of diesel fuel surrogate models, *J. Supercrit. Fluids* 71 (2012) 136–146.
- [35] H.J. Curran, P. Gaffuri, W.J. Pitz, C.K. Westbrook, A comprehensive modeling study of n-heptane oxidation, *Combust. Flame* 114 (1–2) (1998) 149–177.
- [36] V. Golovichev, Mechanisms (combustion chemistry), Chalmers University of Technology, 2013 <http://www.tfd.chalmers.se/~valeri/MECH.html>.
- [37] A. Patel, S.-C. Kong, R.D. Reitz, Development and validation of a reduced reaction mechanism for HCCI engine simulations, *SAE Tech. Paper* (2004).
- [38] W. Pejpichestakul, E. Ranzi, M. Pelucchi, A. Frassoldati, A. Cuoci, A. Parente, T. Faravelli, Examination of a soot model in premixed laminar flames at fuel-rich conditions, *Proc. Combust. Inst.* 37 (1) (2019) 1013–1021.
- [39] A. Stagni, A. Frassoldati, A. Cuoci, T. Faravelli, E. Ranzi, Skeletal mechanism reduction through species-targeted sensitivity analysis, *Combust. Flame* 163 (2016) 382–393.
- [40] M. Mehl, W.J. Pitz, C.K. Westbrook, H.J. Curran, Kinetic modeling of gasoline surrogate components and mixtures under engine conditions, *Proc. Combust. Inst.* 33 (1) (2011) 193–200. %@ 1540-7489.
- [41] M. Mehl, W.J. Pitz, M. Sjöberg, J.E. Dec, Detailed Kinetic Modeling of Low-Temperature Heat Release For PRF Fuels in an HCCI Engine, *SAE Technical Paper*, 2009.
- [42] J.L. Brakora, Y. Ra, R.D. Reitz, J. McFarlane, C.S. Daw, Development and validation of a reduced reaction mechanism for biodiesel-fueled engine simulations, *SAE Int. J. Fuels Lubr.* 1 (1) (2009) 675–702. %@ 1946-3952.
- [43] H.K. Ng, S. Gan, J.-H. Ng, K.M. Pang, Development and validation of a reduced combined biodiesel-diesel reaction mechanism, *Fuel* 104 (2013) 620–634. %@ 0016-2361.
- [44] J.Y. Lai, K.C. Lin, A. Violi, Biodiesel combustion: advances in chemical kinetic modeling, *Prog. Energy Combust. Sci.* 37 (1) (2011) 1–14.
- [45] H.M. Ismail, H.K. Ng, S. Gan, T. Lucchini, A. Onorati, Development of a reduced biodiesel combustion kinetics mechanism for CFD modelling of a light-duty diesel engine, *Fuel* 106 (2013) 388–400.
- [46] K. Seshadri, T. Lu, O. Herbinet, S. Humer, U. Niemann, W.J. Pitz, R. Seiser, C. K. Law, Experimental and kinetic modeling study of extinction and ignition of methyl decanoate in laminar non-premixed flows, *Proc. Combust. Inst.* 32 (1) (2009) 1067–1074. %@ 1540-7489.
- [47] E.M. Fisher, W.J. Pitz, H.J. Curran, C.K. Westbrook, Detailed chemical kinetic mechanisms for combustion of oxygenated fuels, *Proc. Combust. Inst.* 28 (2) (2000) 1579–1586. %@ 1540-7489.
- [48] R. Grana, A. Frassoldati, A. Cuoci, T. Faravelli, E. Ranzi, A wide range kinetic modeling study of pyrolysis and oxidation of methyl butanoate and methyl decanoate. Note I: lumped kinetic model of methyl butanoate and small methyl esters, *Energy* 43 (1) (2012) 124–139. %@ 0360-5442.
- [49] R. Grana, A. Frassoldati, C. Saggese, T. Faravelli, E. Ranzi, A wide range kinetic modeling study of pyrolysis and oxidation of methyl butanoate and methyl decanoate-Note II: lumped kinetic model of decomposition and combustion of methyl esters up to methyl decanoate, *Combust. Flame* 159 (7) (2012) 2280–2294. %@ 0010-2180.
- [50] A. Rodriguez, O. Herbinet, F. Battin-Leclerc, A. Frassoldati, T. Faravelli, E. Ranzi, Experimental and modeling investigation of the effect of the unsaturation degree on the gas-phase oxidation of fatty acid methyl esters found in biodiesel fuels, *Combust. Flame* 164 (2016) 346–362.
- [51] X. Cheng, H.K. Ng, S. Gan, J.H. Ho, K.M. Pang, Development and validation of a generic reduced chemical kinetic mechanism for CFD spray combustion modelling of biodiesel fuels, *Combust. Flame* 162 (6) (2015) 2354–2370.
- [52] Y. Chen, T. Chen, Y. Feng, J.I. Ryu, H. Yang, J.-Y. Chen, H radical sensitivity-assisted automatic chemical kinetic model reduction for laminar flame chemistry retaining: a case study of gasoline-DME mixture under engine conditions, *Energy Fuels* 33 (4) (2019) 3551–3556.
- [53] Y. Wu, P. Pal, S. Som, T. Lu, A skeletal chemical kinetic mechanism for gasoline and gasoline/ethanol blend surrogates for engine CFD applications, in: *International Conference on Chemical Kinetics*, 2017.
- [54] M. Mehl, J.-Y. Chen, W.J. Pitz, S.M. Sarathy, C.K. Westbrook, An approach for formulating surrogates for gasoline with application toward a reduced surrogate mechanism for CFD engine modeling, *Energy Fuels* 25 (11) (2011) 5215–5223.
- [55] Y. Chen, B. Wolk, M. Mehl, W.K. Cheng, J.-Y. Chen, R.W. Dibble, Development of a reduced chemical mechanism targeted for a 5-component gasoline surrogate: a case study on the heat release nature in a GCI engine, *Combust. Flame* 178 (2017) 268–276. %@ 0010-2180.
- [56] G. Kukkadapu, K. Kumar, C.-J. Sung, M. Mehl, W.J. Pitz, Autoignition of gasoline and its surrogates in a rapid compression machine, *Proc. Combust. Inst.* 34 (1) (2013) 345–352.
- [57] G. Kukkadapu, K. Kumar, C.-J. Sung, M. Mehl, W.J. Pitz, Experimental and surrogate modeling study of gasoline ignition in a rapid compression machine, *Combust. Flame* 159 (10) (2012) 3066–3078.
- [58] P. Kundu, C. Xu, S. Som, J. Temme, C.-B.M. Kweon, S. Lapointe, G. Kukkadapu, W. J. Pitz, Implementation of multi-component diesel fuel surrogates and chemical kinetic mechanisms for engine combustion simulations, *Transp. Eng.* 3 (2021), 100042.
- [59] Y. Li, A. Alfazazi, B. Mohan, E.A. Tingas, J. Badra, H.G. Im, S.M. Sarathy, Development of a reduced four-component (toluene/n-heptane/iso-octane/ethanol) gasoline surrogate model, *Fuel* 247 (2019) 164–178.
- [60] Y. Pei, M. Mehl, W. Liu, T. Lu, W.J. Pitz, S. Som, A multicomponent blend as a diesel fuel surrogate for compression ignition engine applications, *J. Eng. Gas Turbine Power* 137 (11) (2015).
- [61] G. Wu, X. Wang, S. Abubakar, Y. Li, Z. Liu, A realistic skeletal mechanism for the oxidation of biodiesel surrogate composed of long carbon chain and polyunsaturated compounds, *Fuel* 289 (2021), 119934.
- [62] D. Alviso, M.W. Costa, L. Backer, P. Pepiot, N. Darabiha, R.G. dos Santos, Chemical kinetic mechanism for diesel/biodiesel/ethanol surrogates using n-decane/methyl-decanoate/ethanol blends, *J. Braz. Soc. Mecha. Sci. Eng.* 42 (2) (2020) 1–14.
- [63] K.E. Niemeyer, C.-J. Sung, Mechanism reduction for multicomponent surrogates: a case study using toluene reference fuels, *Combust. Flame* 161 (11) (2014) 2752–2764. %@ 0010-2180.
- [64] A.R. Martins, A.I. Ferreira, R. Segurado, M.A. Mendes, Reduced Reaction Model for Secondary Gas Phase in Biomass Gasification, *Energy Fuels* (2021).
- [65] J.W. Jung, Y.C. Lim, H.K. Suh, A study on the mechanism reduction and evaluation of biodiesel with the change of mechanism reduction factors, *Proc. Inst. Mech. Eng. Part D J. Automob. Eng.* 234 (14) (2020) 3398–3413.
- [66] T. Nagy, T. Turányi, Reduction of very large reaction mechanisms using methods based on simulation error minimization, *Combust. Flame* 156 (2) (2009) 417–428.
- [67] T. Lu, C.K. Law, On the applicability of directed relation graphs to the reduction of reaction mechanisms, *Combust. Flame* 146 (3) (2006) 472–483.

- [68] S. Lin, M. Xie, J. Wang, W. Liang, C.K. Law, W. Zhou, B. Yang, Chemical kinetic model reduction through species-targeted global sensitivity analysis (STGSA), *Combust. Flame* 224 (2021) 73–82.
- [69] Y. Chang, M. Jia, B. Niu, X. Dong, P. Wang, Reduction of large-scale chemical mechanisms using global sensitivity analysis on reaction class/sub-mechanism, *Combust. Flame* 212 (2020) 355–366.
- [70] R. Li, S. Li, F. Wang, X. Li, Sensitivity analysis based on intersection approach for mechanism reduction of cyclohexane, *Combust. Flame* 166 (2016) 55–65.
- [71] V. Dias, H.M. Katshiatshia, H. Jeanmart, The influence of ethanol addition on a rich premixed benzene flame at low pressure, *Combust. Flame* 161 (9) (2014) 2297–2304.
- [72] M.B. Colket III, L.J. Spadaccini, Scramjet fuels autoignition study, *J. Propul. Power* 17 (2) (2001) 315–323.
- [73] R. Grana, A. Frassoldati, A. Cuoci, T. Faravelli, E. Ranzi, A wide range kinetic modeling study of pyrolysis and oxidation of methyl butanoate and methyl decanoate. Note I: lumped kinetic model of methyl butanoate and small methyl esters, *Energy* 43 (1) (2012) 124–139.
- [74] R. Grana, A. Frassoldati, C. Saggese, T. Faravelli, E. Ranzi, A wide range kinetic modeling study of pyrolysis and oxidation of methyl butanoate and methyl decanoate—Note II: lumped kinetic model of decomposition and combustion of methyl esters up to methyl decanoate, *Combust. Flame* 159 (7) (2012) 2280–2294.
- [75] W. Sang, Knock Mitigation On Boosted Controlled Auto-Ignition Engines With Fuel Stratification and Exhaust Gas Recycling, Massachusetts Institute of Technology, 2013.
- [76] Corn- 26 P. Dagaut, M. Reuillon, M. Cathonnet, Y. Hidaka, K. Kimura, H. Kawano, *Combust. Bust. Sci. Technol.* 95 (1994) 233.
- [77] P. Dagaut, M. Reuillon, M. Cathonnet, Experimental study of the oxidation of n-heptane in a jet stirred reactor from low to high temperature and pressures up to 40 atm, *Combust. Flame* 101 (1–2) (1995) 132–140.